APPENDIX A

IMAGES OF CERCHAR STYLUS TIPS AND THEIR CORRESPONDING GROOVES

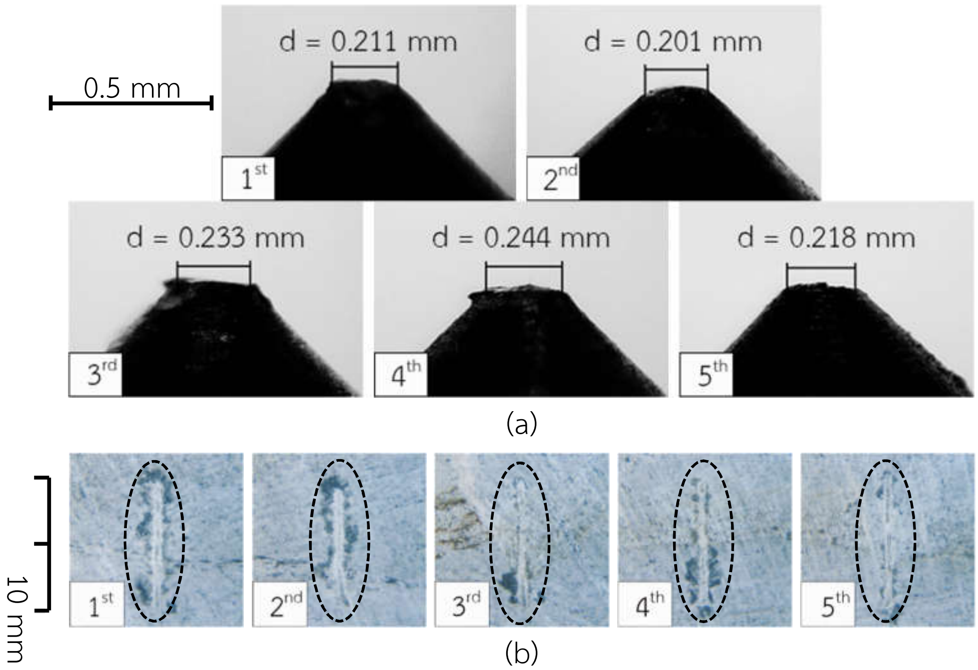

Figure A.1 Close-up images of stylus tip after scratching on Khao Khad argillaceous limestone with α = 0° (a) and their corresponding groove images (b).

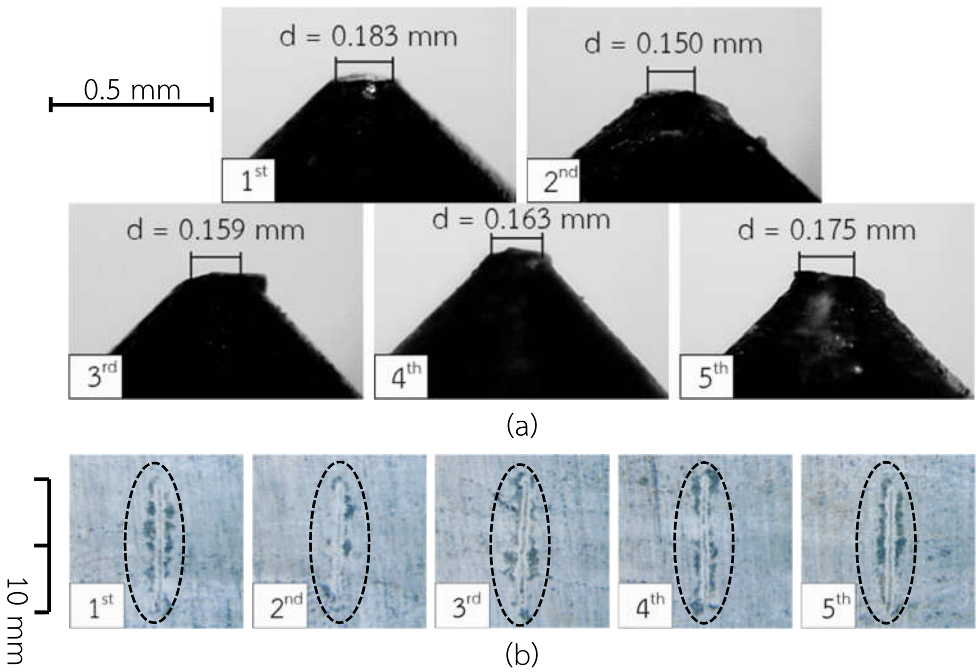

Figure A.2 Close-up images of stylus tip after scratching on Khao Khad argillaceous limestone with α = 45°, θ = 90° (a) and their corresponding groove images (b).

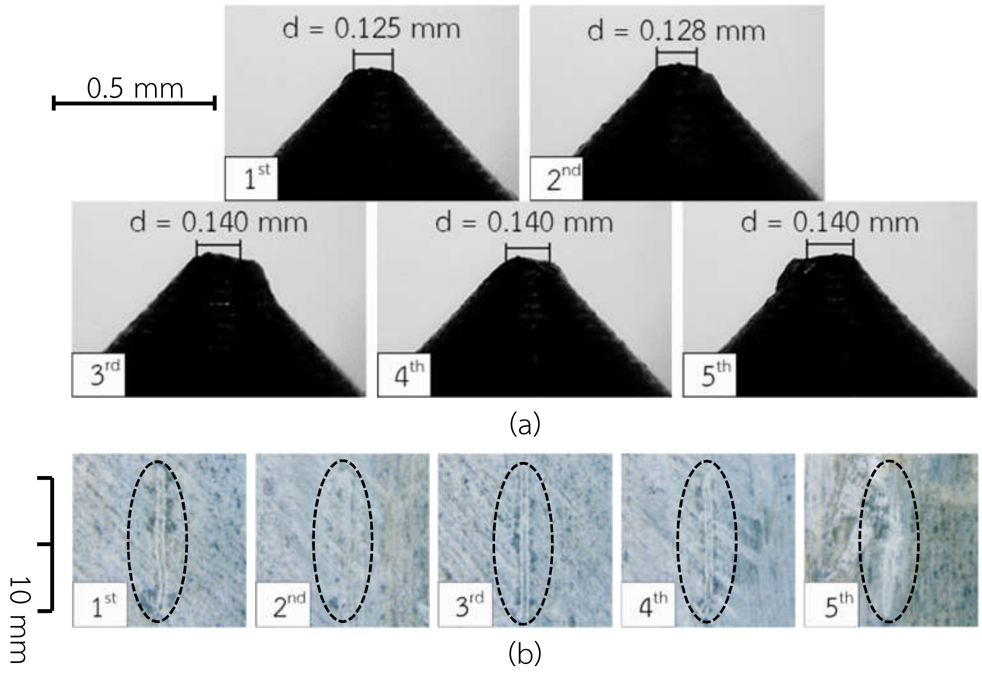

Figure A.3 Close-up images of stylus tip after scratching on Khao Khad argillaceous limestone with α = 90°, θ = 0° (a) and their corresponding groove images (b).

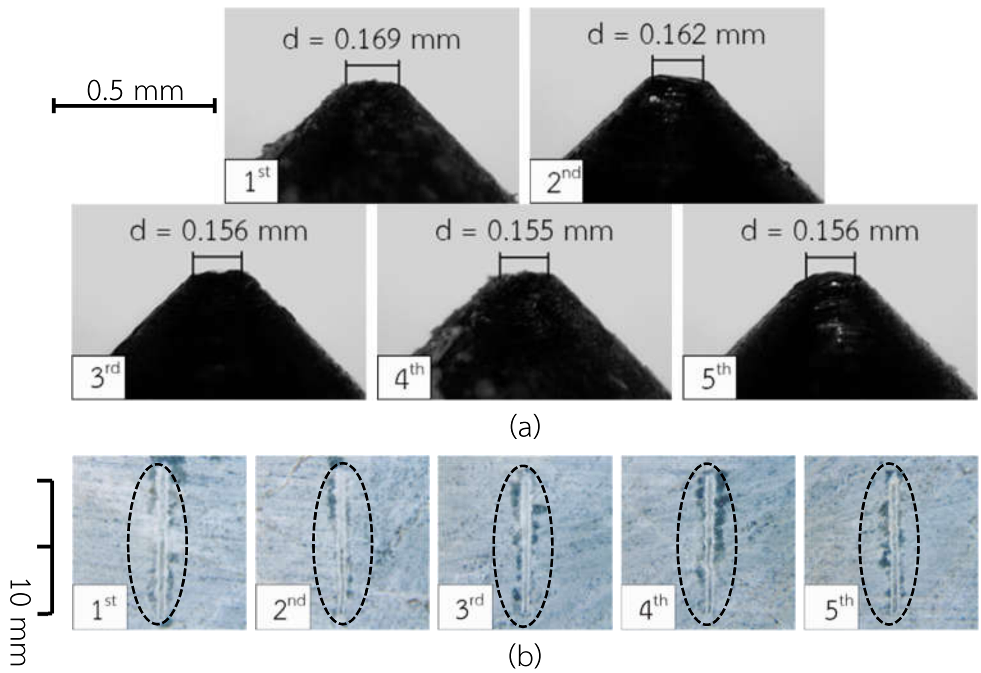

Figure A.4 Close-up images of stylus tip after scratching on Khao Khad argillaceous limestone with α = 90°, θ = 45° (a) and their corresponding groove images (b).

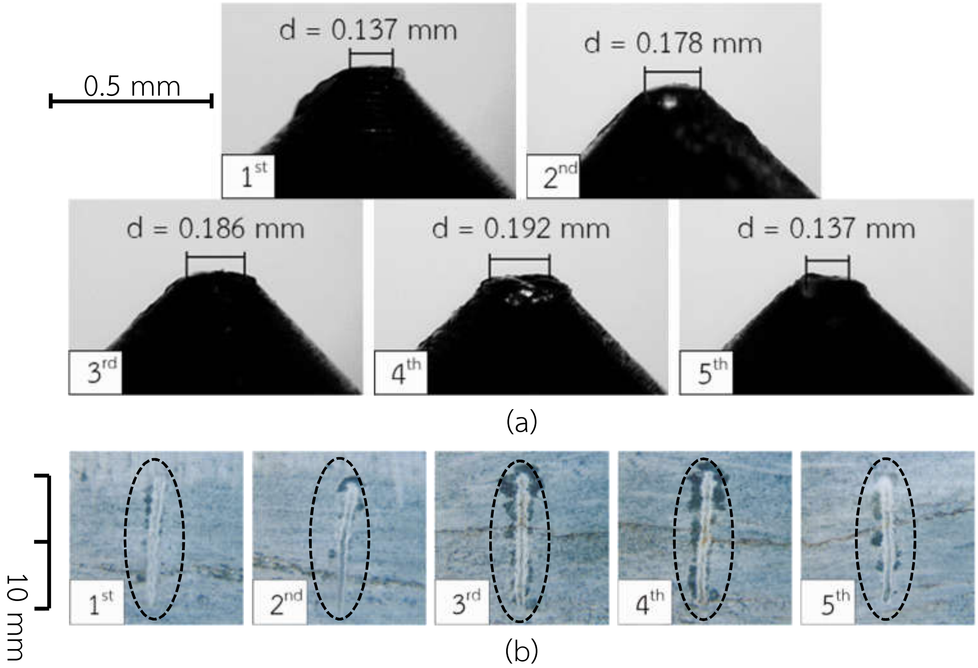

Figure A.5 Close-up images of stylus tip after scratching on Khao Khad argillaceous limestone with α = 90°, θ = 90° (a) and their corresponding groove images (b).

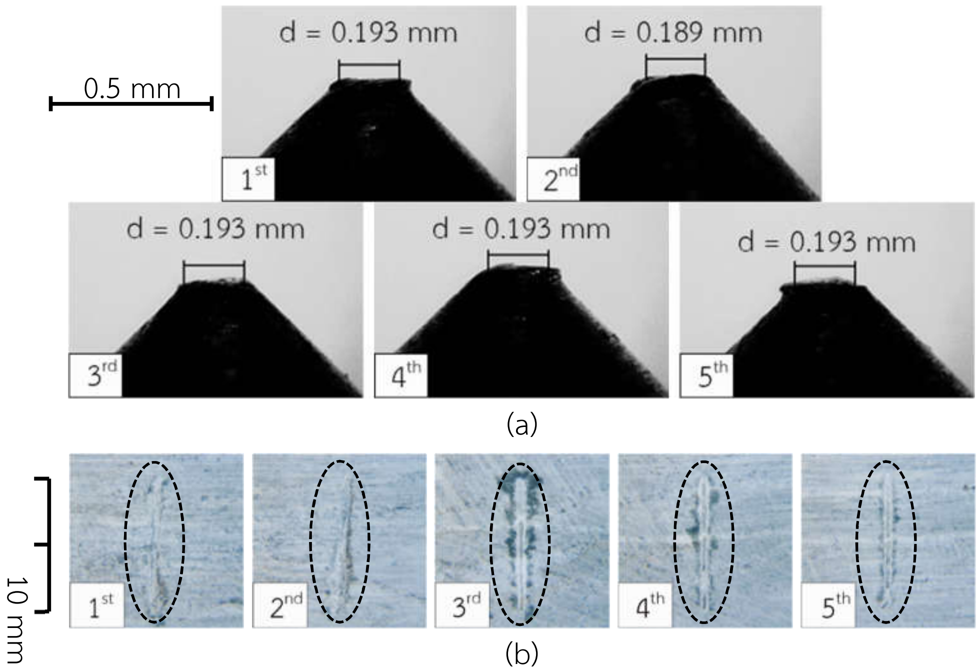

Figure A.6 Close-up images of stylus tip after scratching on Khao Khad argillaceous limestone with α = 135°, θ = 90° (a) and their corresponding groove images (b).

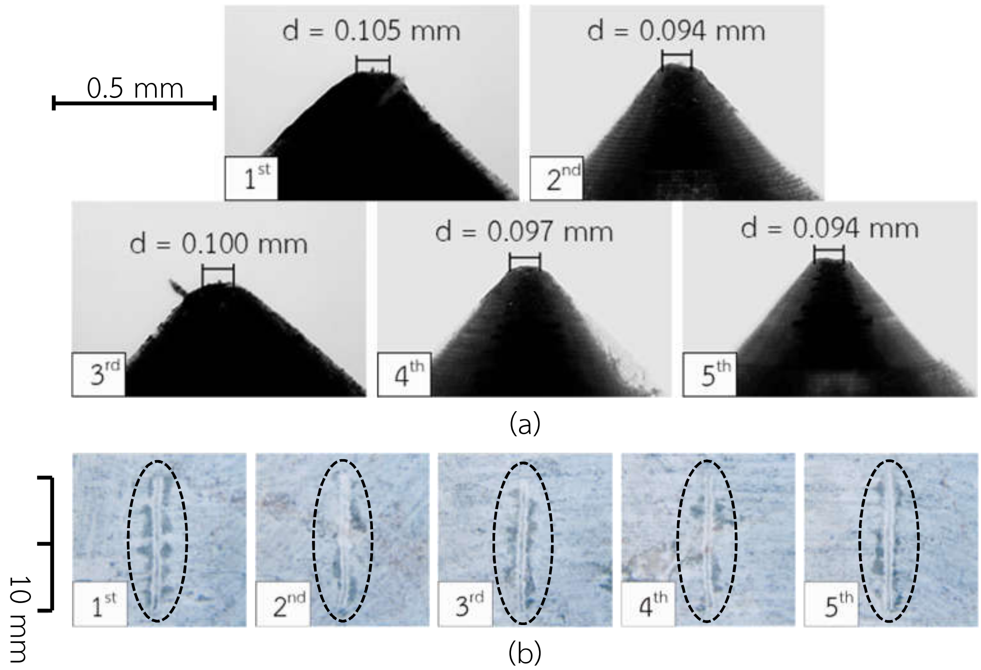

Figure A.7 Close-up images of stylus tip after scratching on Khao Khad bedded limestone with α = 0° (a) and their corresponding groove images (b).

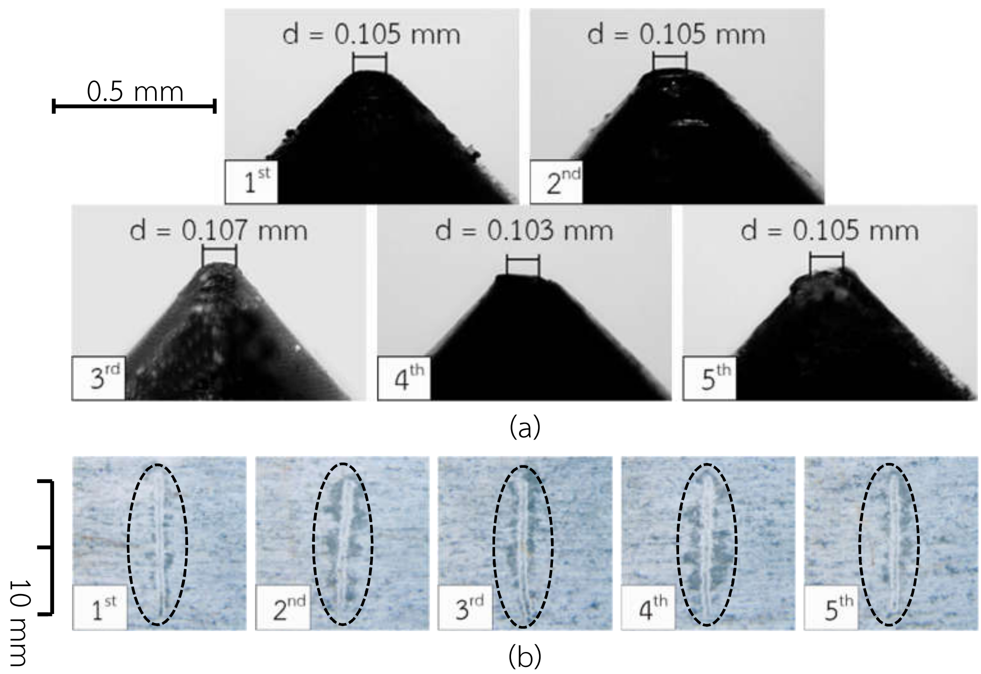

Figure A.8 Close-up images of stylus tip after scratching on Khao Khad bedded limestone with α = 45°, θ = 90° (a) and their corresponding groove images (b).

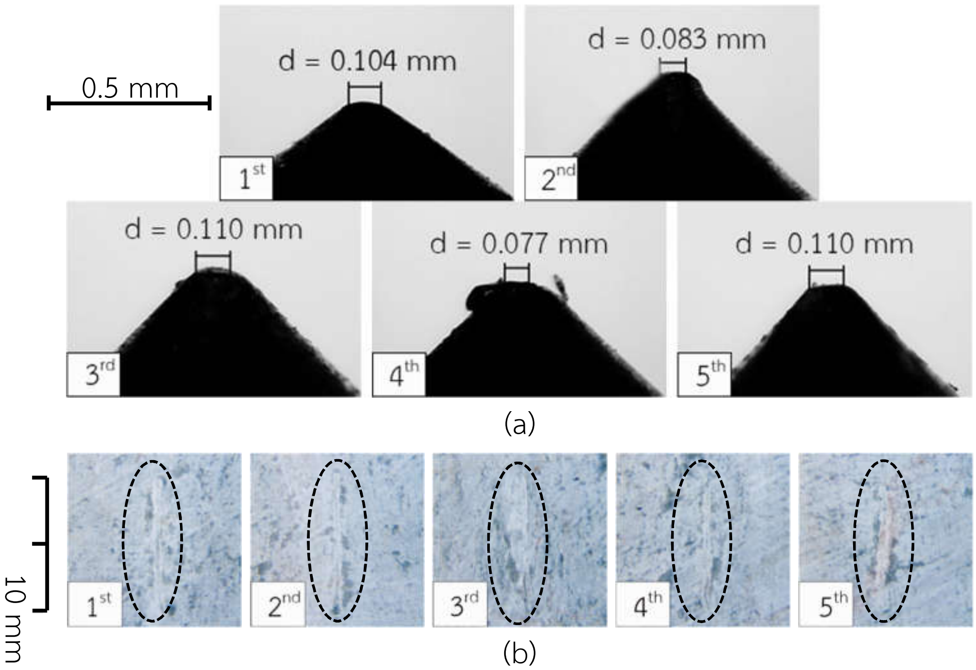

Figure A.9 Close-up images of stylus tip after scratching on Khao Khad bedded limestone with α = 90°, θ = 0° (a) and their corresponding groove images (b).

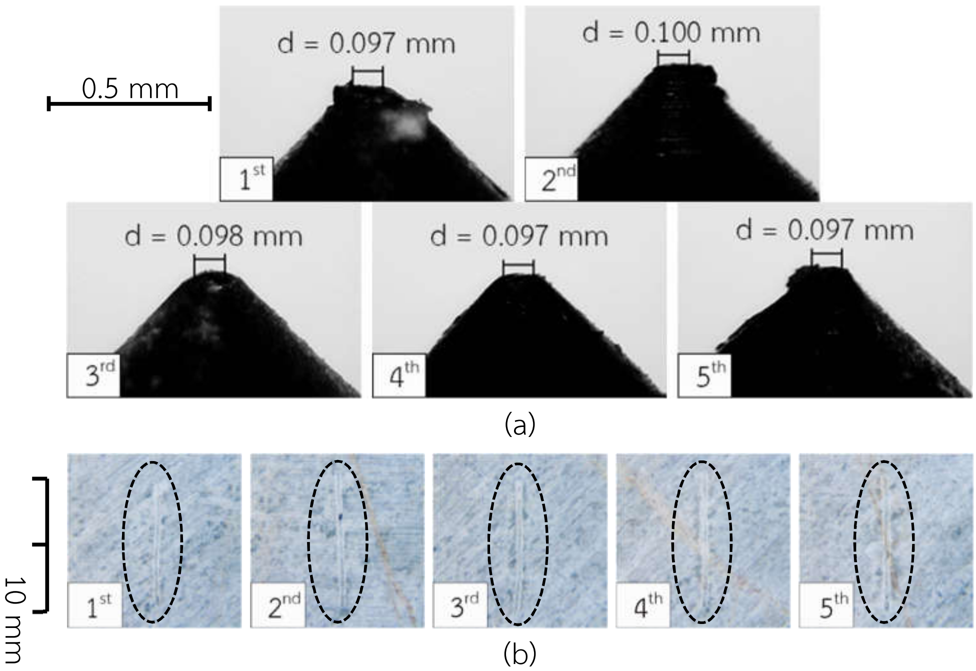

Figure A.10 Close-up images of stylus tip after scratching on Khao Khad bedded limestone with α = 90°, θ = 45° (a) and their corresponding groove images (b).

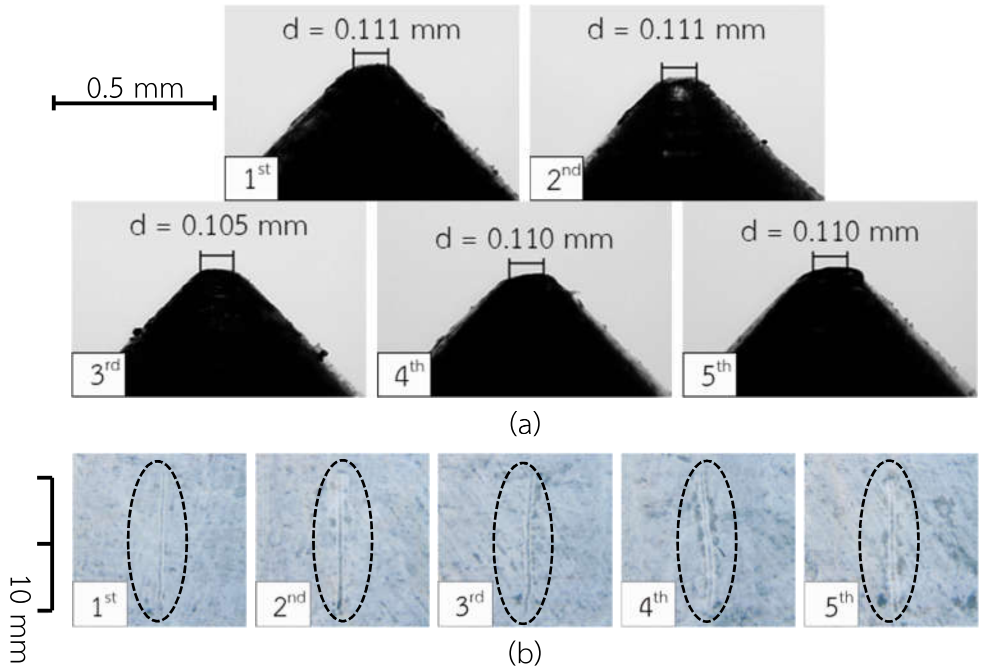

Figure A.11 Close-up images of stylus tip after scratching on Khao Khad bedded limestone with α = 90°, θ = 90° (a) and their corresponding groove images (b).

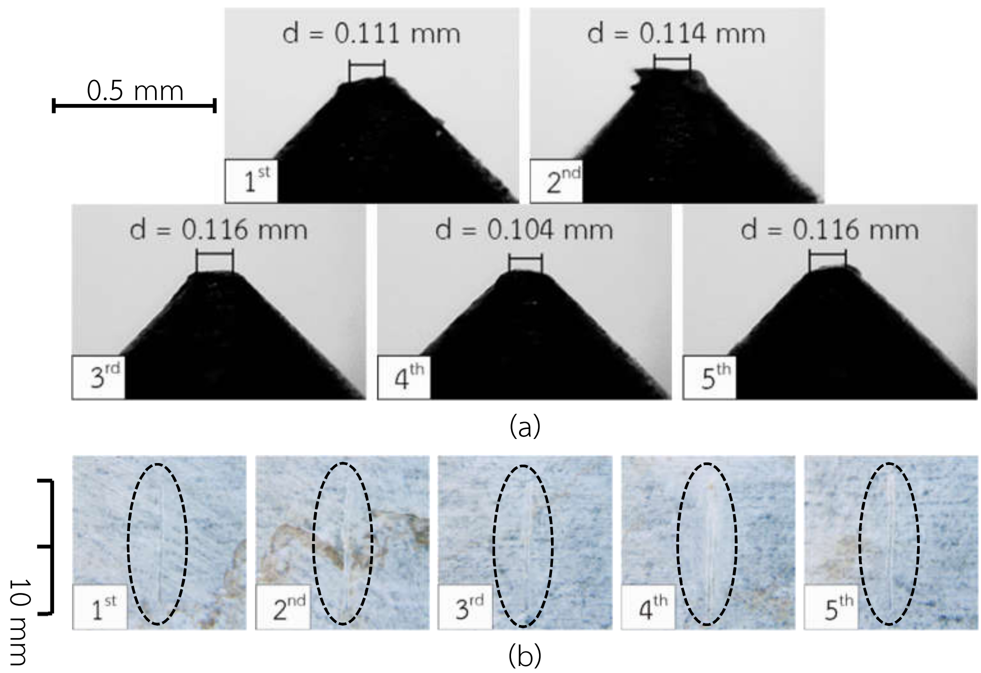

Figure A.12 Close-up images of stylus tip after scratching on Khao Khad bedded limestone with α = 135°, θ = 90° (a) and their corresponding groove images (b).

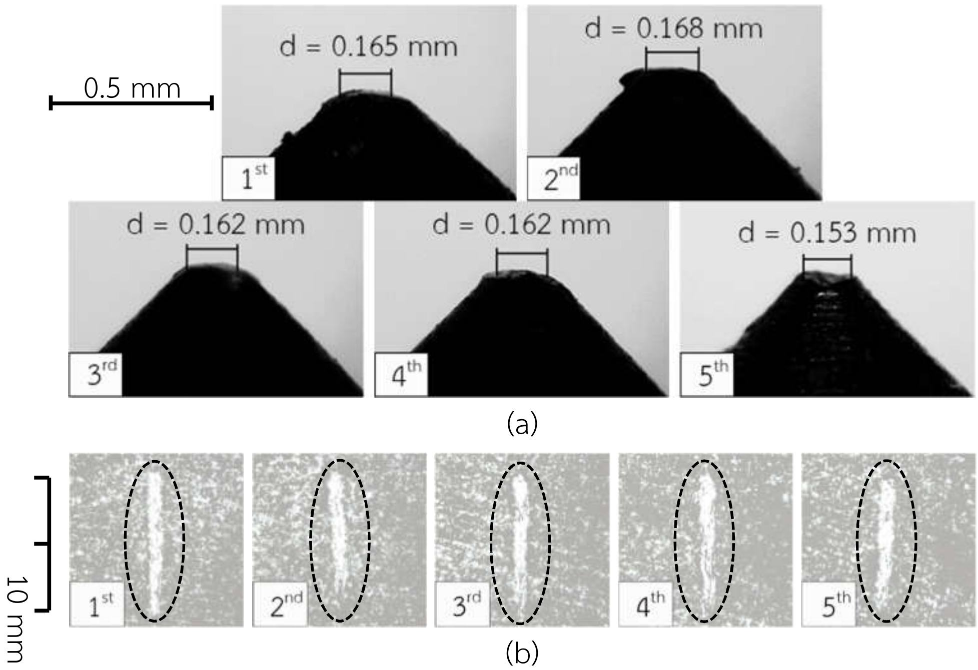

Figure A.13 Close-up images of stylus tip after scratching on Phu Kadueng sandstone with α = 0° (a) and their corresponding groove images (b).

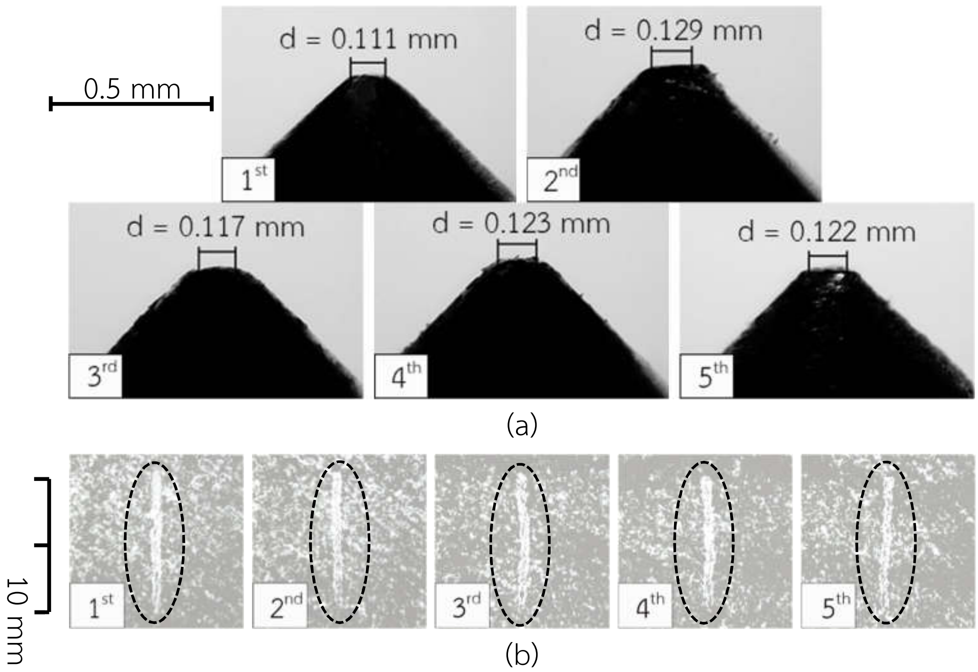

Figure A.14 Close-up images of stylus tip after scratching on Phu Kadueng sandstone with α = 45°, θ = 90° (a) and their corresponding groove images (b).

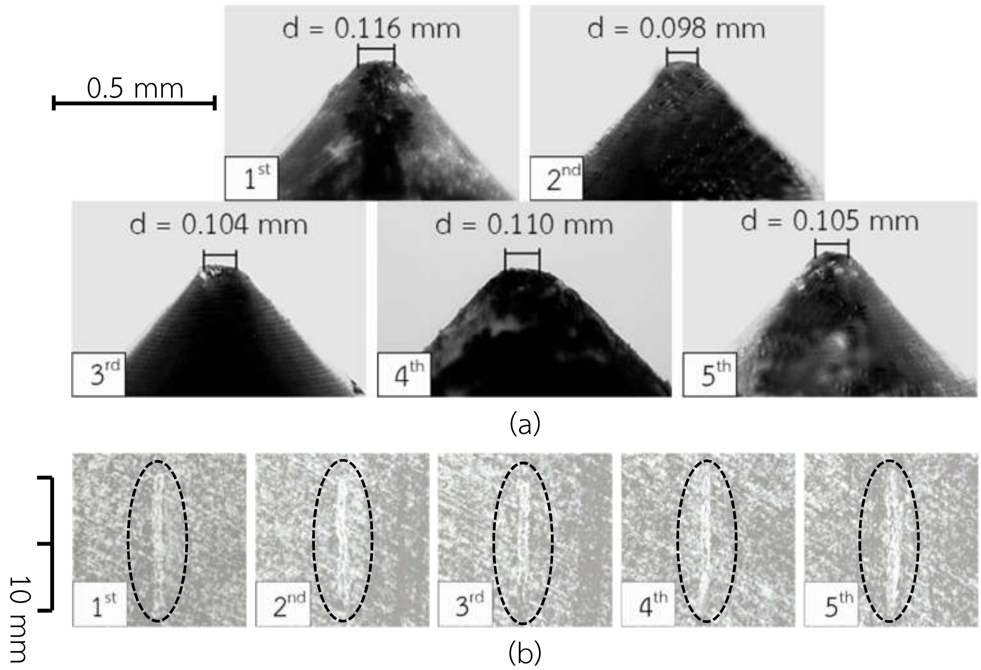

Figure A.15 Close-up images of stylus tip after scratching on Phu Kadueng sandstone with α = 90°, θ = 0° (a) and their corresponding groove images (b).

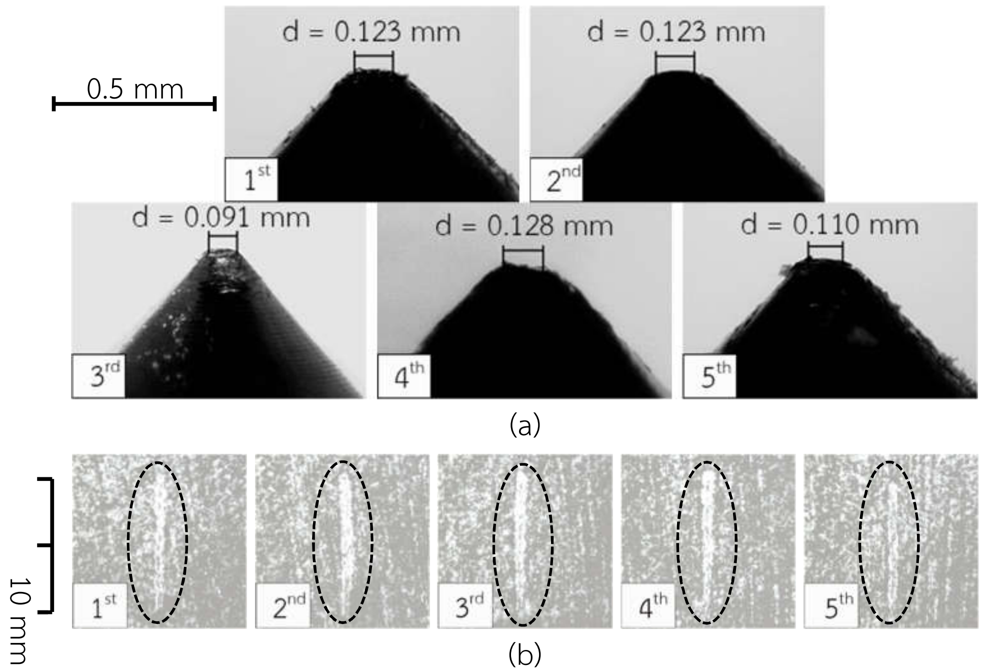

Figure A.16 Close-up images of stylus tip after scratching on Phu Kadueng sandstone with α = 90°, θ = 45° (a) and their corresponding groove images (b).

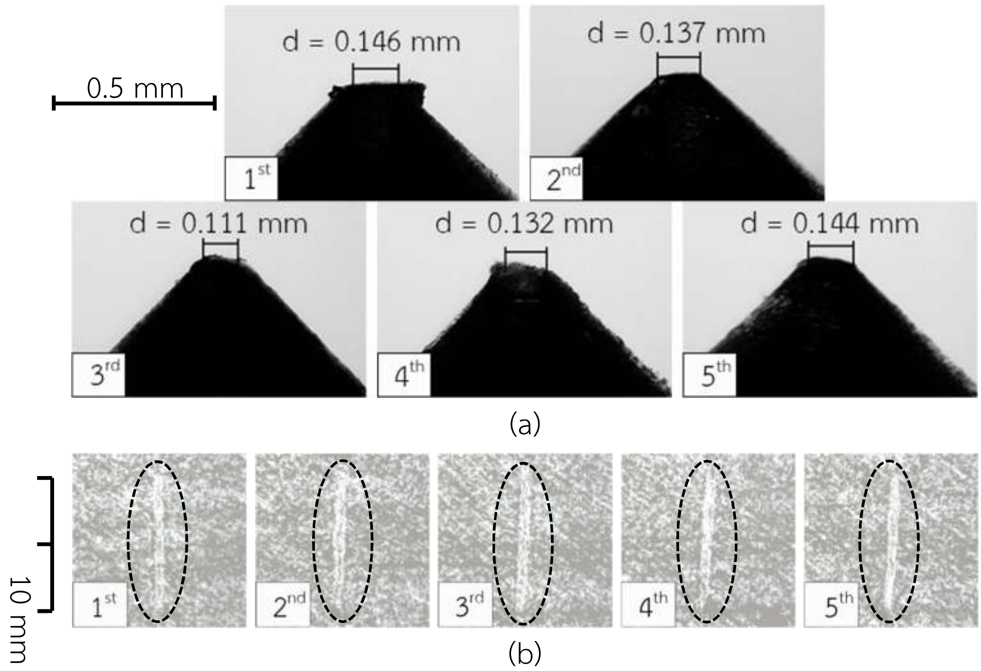

Figure A.17 Close-up images of stylus tip after scratching on Phu Kadueng sandstone with α = 90°, θ = 90° (a) and their corresponding groove images (b).

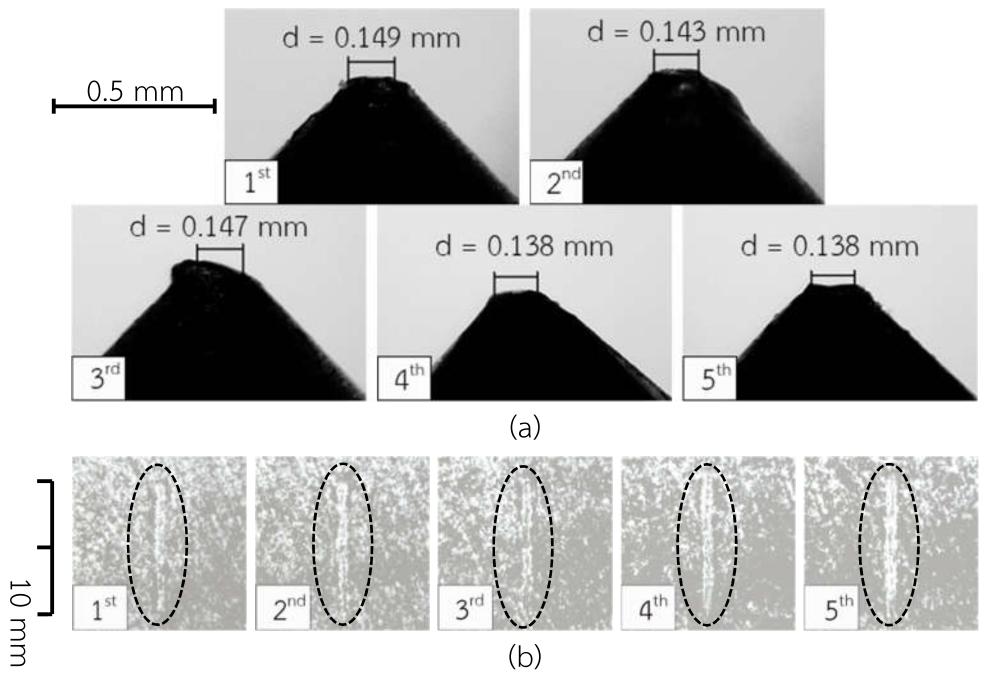

Figure A.18 Close-up images of stylus tip after scratching on Phu Kadueng sandstone with α = 135°, θ = 90° (a) and their corresponding groove images (b).

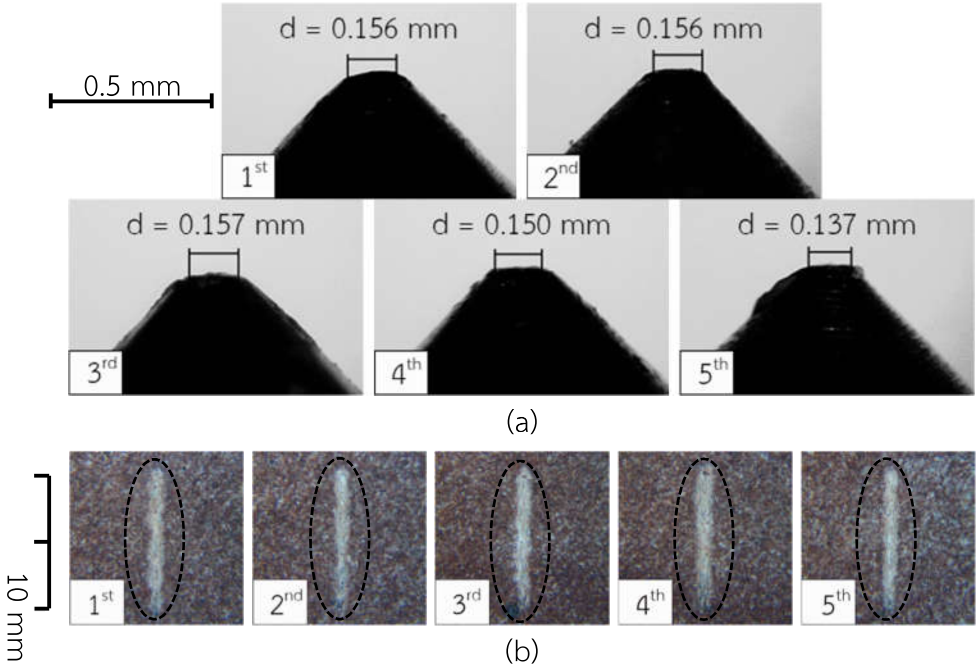

Figure A.19 Close-up images of stylus tip after scratching on Phu Phan sandstone with α = 0° (a) and their corresponding groove images (b).

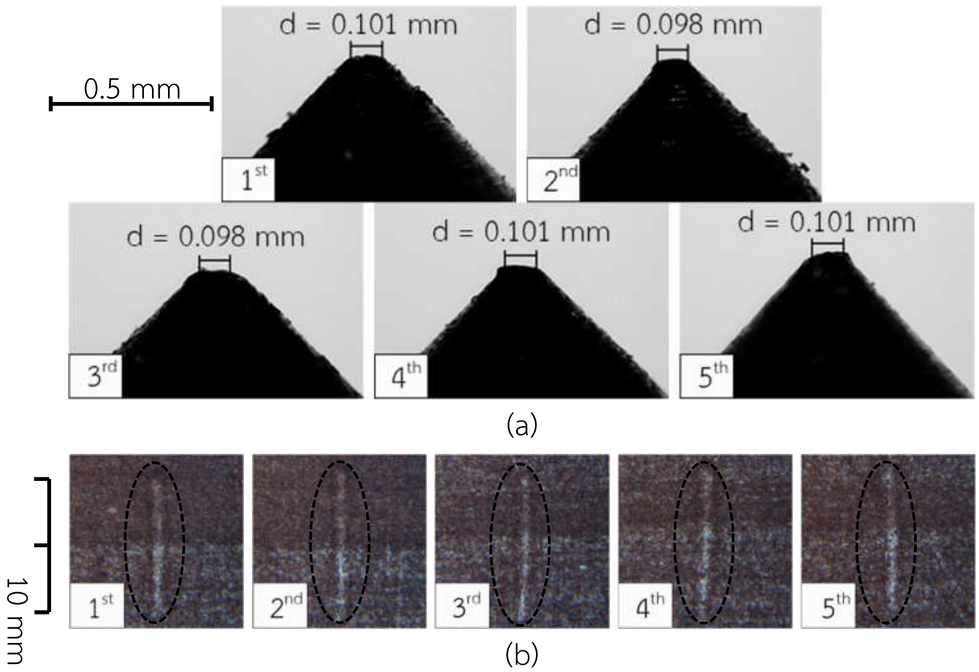

Figure A.20 Close-up images of stylus tip after scratching on Phu Phan sandstone with α = 45°, θ = 90° (a) and their corresponding groove images (b).

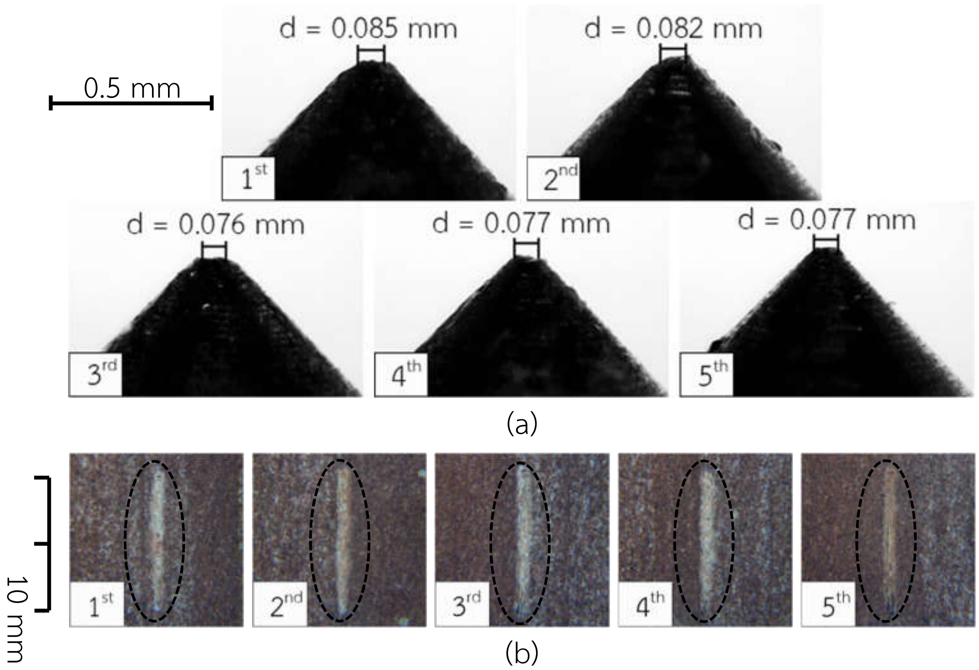

Figure A.21 Close-up images of stylus tip after scratching on Phu Phan sandstone with α = 90°, θ = 0° (a) and their corresponding groove images (b).

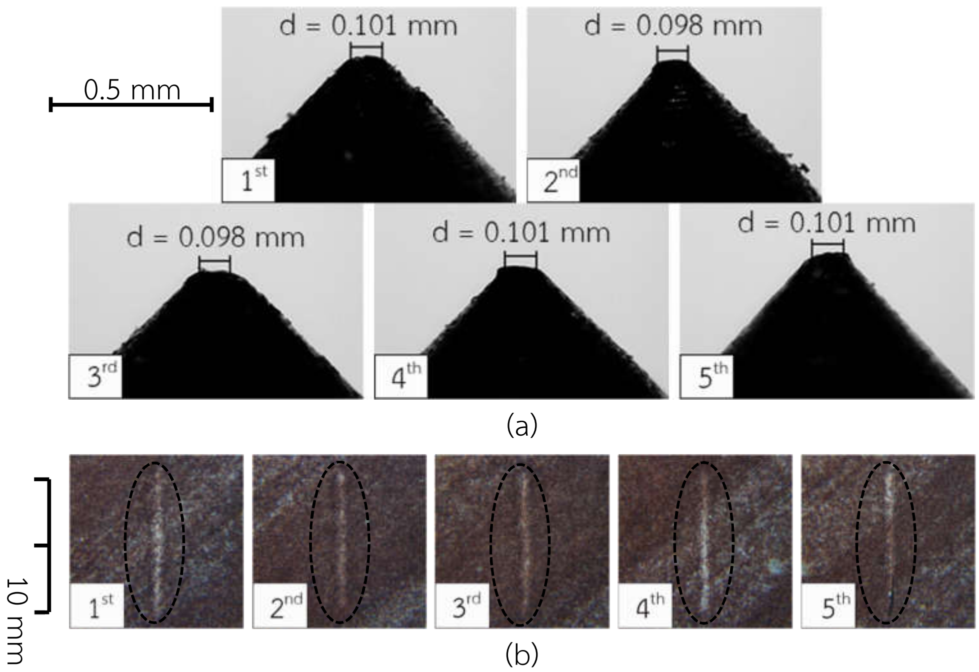

Figure A.22 Close-up images of stylus tip after scratching on Phu Phan sandstone with α = 90°, θ = 45° (a) and their corresponding groove images (b).

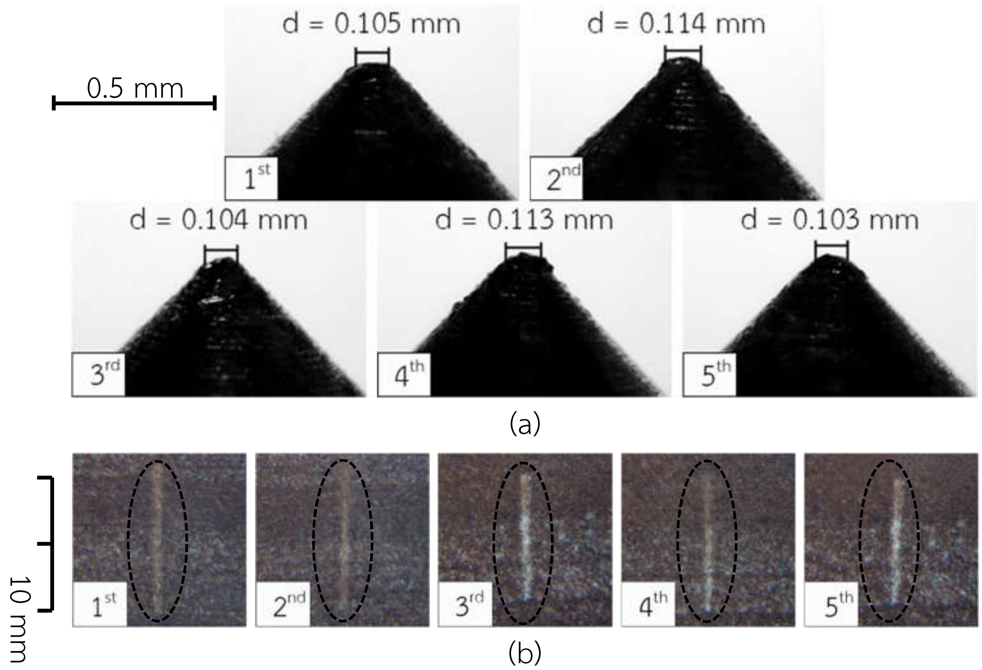

Figure A.23 Close-up images of stylus tip after scratching on Phu Phan sandstone with α = 90°, θ = 90° (a) and their corresponding groove images (b).

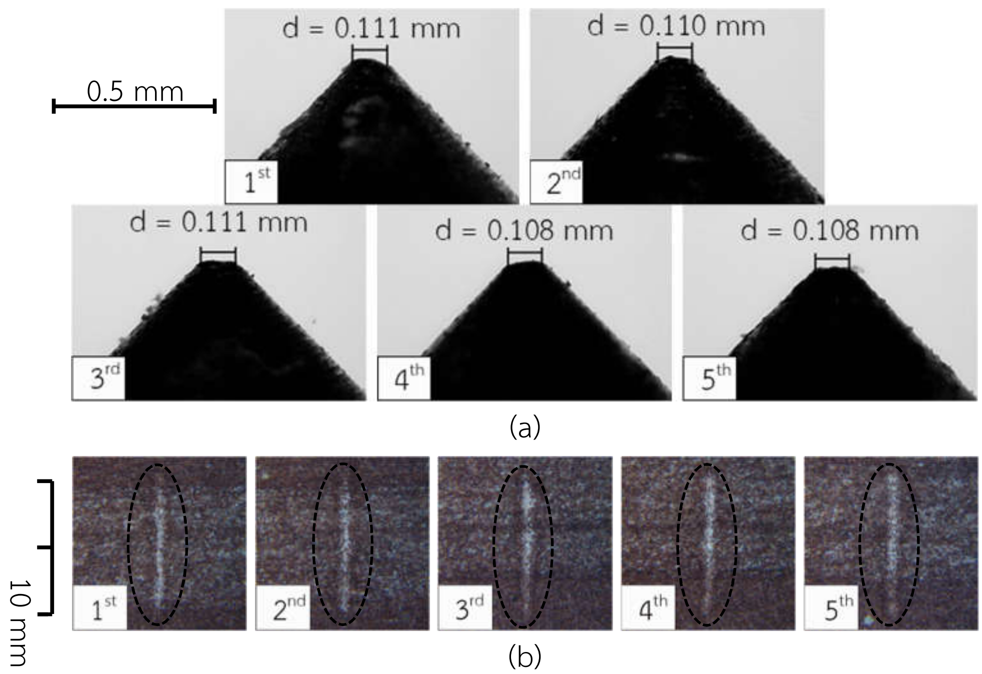

Figure A.24 Close-up images of stylus tip after scratching on Phu Phan sandstone with α = 135°, θ = 90° (a) and their corresponding groove images (b).

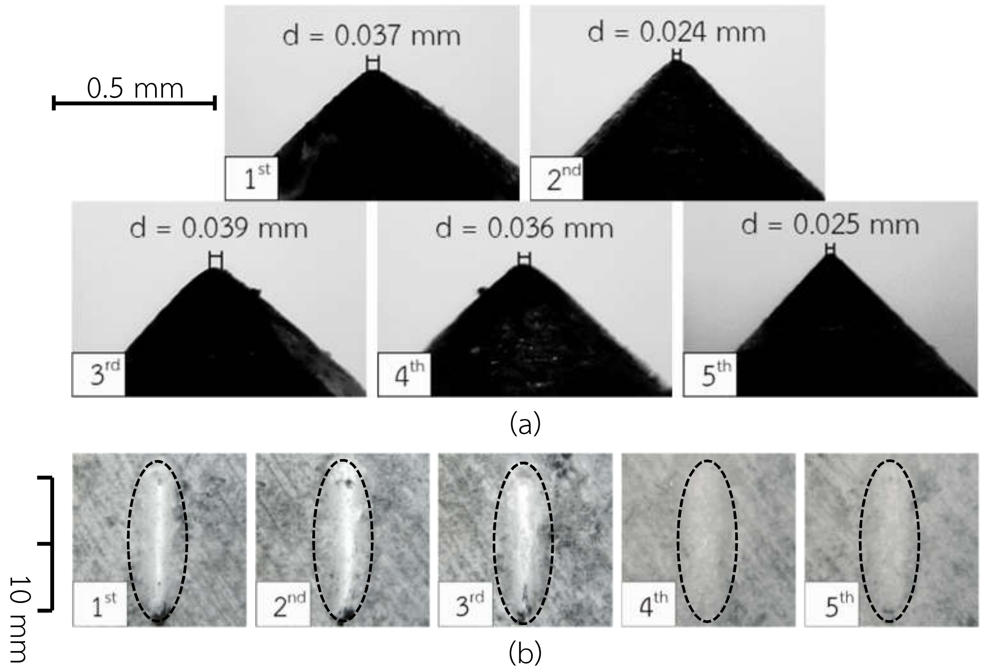

Figure A.25 Close-up images of stylus tip after scratching on Tak Fa gypsum with α = 0° (a) and their corresponding groove images (b).

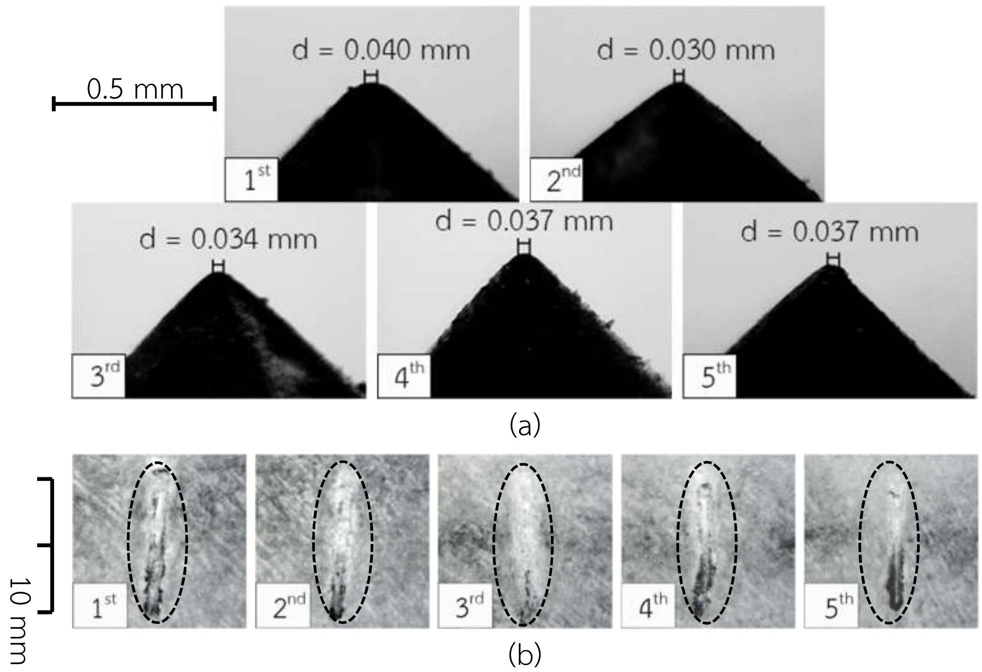

Figure A.26 Close-up images of stylus tip after scratching on Tak Fa gypsum with α = 45°, θ = 90° (a) and their corresponding groove images (b).

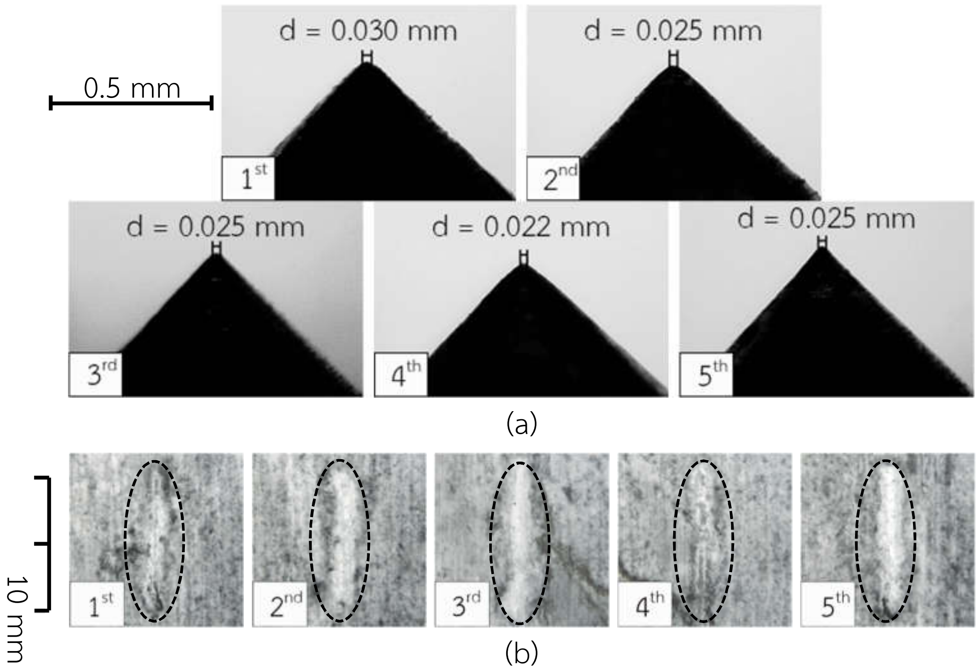

Figure A.27 Close-up images of stylus tip after scratching on Tak Fa gypsum with α = 90°, θ = 0° (a) and their corresponding groove images (b).

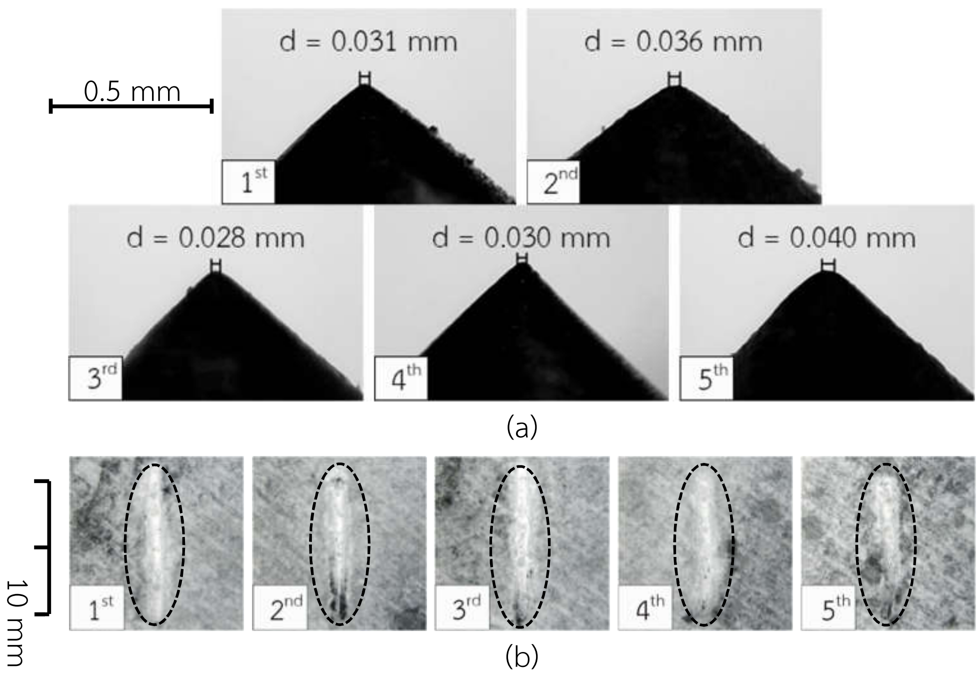

Figure A.28 Close-up images of stylus tip after scratching on Tak Fa gypsum with α = 90°, θ = 45° (a) and their corresponding groove images (b).

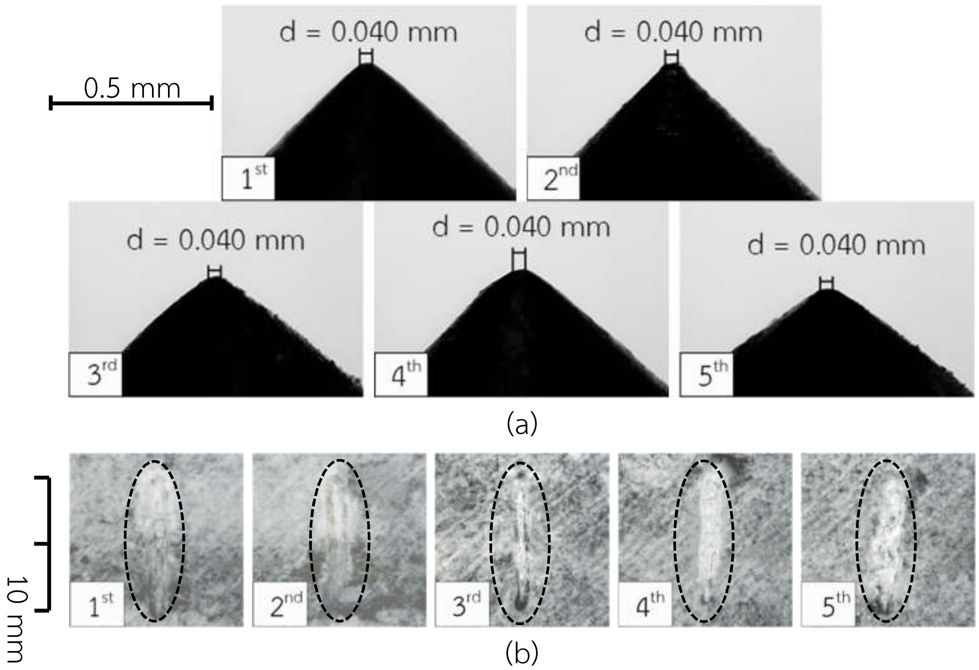

Figure A.29 Close-up images of stylus tip after scratching on Tak Fa gypsum with α = 90°, θ = 90° (a) and their corresponding groove images (b).

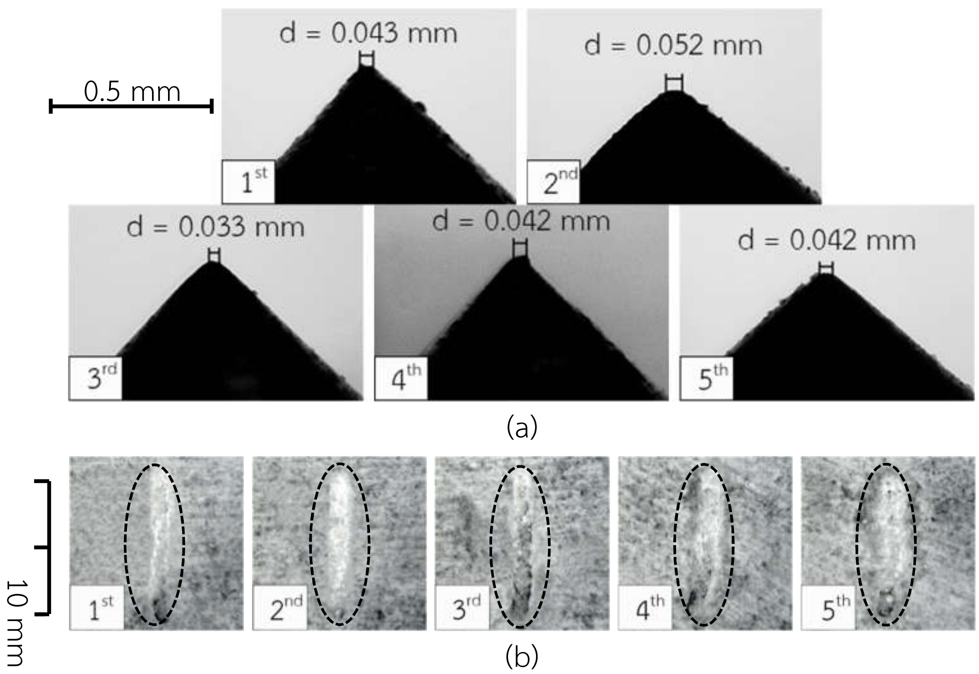

Figure A.30 Close-up images of stylus tip after scratching on Tak Fa gypsum with α = 135°, θ = 90° (a) and their corresponding groove images (b).

APPENDIX B

CERCHAR TEST RESULTS

Table B.1 Measurement results of stylus tip wear at four directions on Khao Khad argillaceous limestone.

α (degrees)	θ (degrees)	Lines	d (mm)					
			Front	Left	Right	Back	Average	SD
0	-	1st	0.211	0.211	0.211	0.211	0.211	0.000
		2nd	0.233	0.201	0.195	0.230	0.215	0.017
		3rd	0.244	0.229	0.233	0.244	0.238	0.007
		4th	0.257	0.193	0.227	0.244	0.230	0.024
		5th	0.218	0.218	0.218	0.218	0.218	0.000
45	90	1st	0.183	0.150	0.150	0.180	0.166	0.016
		2nd	0.175	0.150	0.152	0.165	0.161	0.010
		3rd	0.168	0.162	0.159	0.162	0.163	0.003
		4th	0.171	0.163	0.149	0.169	0.163	0.009
		5th	0.175	0.155	0.152	0.171	0.163	0.010
90	0	1st	0.149	0.125	0.135	0.148	0.139	0.010
		2nd	0.148	0.128	0.135	0.148	0.140	0.009
		3rd	0.142	0.142	0.140	0.142	0.142	0.001
		4th	0.143	0.141	0.140	0.142	0.142	0.001
		5th	0.149	0.138	0.136	0.145	0.142	0.005
90	45	1st	0.169	0.146	0.146	0.160	0.155	0.010
		2nd	0.162	0.160	0.141	0.162	0.156	0.009
		3rd	0.156	0.141	0.156	0.156	0.152	0.006
		4th	0.162	0.149	0.155	0.155	0.155	0.005
		5th	0.163	0.149	0.149	0.156	0.154	0.006
90	90	1st	0.186	0.175	0.163	0.181	0.176	0.009
		2nd	0.183	0.166	0.144	0.178	0.168	0.015
		3rd	0.186	0.165	0.169	0.180	0.175	0.008
		4th	0.193	0.143	0.181	0.192	0.177	0.020
		5th	0.201	0.180	0.137	0.189	0.177	0.024
135	90	1st	0.193	0.193	0.193	0.193	0.193	0.000
		2nd	0.212	0.189	0.163	0.204	0.192	0.019
		3rd	0.194	0.193	0.192	0.194	0.193	0.001
		4th	0.195	0.192	0.191	0.192	0.193	0.002
		5th	0.194	0.192	0.192	0.194	0.193	0.001

Table B.2 Measurement results of stylus tip wear at four directions on Khao Khad bedded limestone.

α (degrees)	θ (degrees)	Lines	d (mm)					
			Front	Left	Right	Back	Average	SD
0	-	1st	0.105	0.102	0.103	0.103	0.103	0.001
		2nd	0.107	0.105	0.094	0.106	0.103	0.005
		3rd	0.105	0.096	0.100	0.105	0.102	0.004
		4th	0.106	0.097	0.099	0.105	0.102	0.004
		5th	0.105	0.102	0.094	0.105	0.102	0.005
45	90	1st	0.108	0.104	0.104	0.105	0.105	0.002
		2nd	0.105	0.105	0.105	0.105	0.105	0.000
		3rd	0.108	0.106	0.105	0.107	0.107	0.001
		4th	0.106	0.103	0.103	0.105	0.104	0.001
		5th	0.105	0.105	0.105	0.105	0.105	0.000
90	0	1st	0.104	0.080	0.095	0.095	0.094	0.009
		2nd	0.110	0.091	0.083	0.095	0.095	0.010
		3rd	0.110	0.086	0.079	0.095	0.093	0.012
		4th	0.105	0.095	0.077	0.100	0.094	0.011
		5th	0.110	0.071	0.086	0.107	0.094	0.016
90	45	1st	0.100	0.086	0.097	0.100	0.096	0.006
		2nd	0.100	0.092	0.094	0.100	0.097	0.004
		3rd	0.101	0.092	0.097	0.098	0.097	0.003
		4th	0.097	0.097	0.097	0.097	0.097	0.000
		5th	0.097	0.097	0.097	0.097	0.097	0.000
90	90	1st	0.111	0.111	0.111	0.111	0.111	0.000
		2nd	0.111	0.111	0.111	0.111	0.111	0.000
		3rd	0.111	0.105	0.111	0.111	0.110	0.003
		4th	0.110	0.110	0.110	0.110	0.110	0.000
		5th	0.112	0.109	0.109	0.110	0.110	0.001
135	90	1st	0.119	0.111	0.111	0.111	0.113	0.003
		2nd	0.114	0.105	0.110	0.111	0.110	0.003
		3rd	0.116	0.104	0.116	0.116	0.113	0.005
		4th	0.117	0.104	0.115	0.115	0.113	0.005
		5th	0.116	0.105	0.102	0.116	0.110	0.006

Table B.3 Measurement results of stylus tip wear at four directions on Phu Kadueng sandstone.

α (degrees)	θ (degrees)	Lines	d (mm)					
			Front	Left	Right	Back	Average	SD
0	-	1st	0.168	0.162	0.165	0.165	0.165	0.002
		2nd	0.170	0.166	0.166	0.168	0.168	0.002
		3rd	0.170	0.162	0.160	0.170	0.166	0.005
		4th	0.172	0.165	0.162	0.170	0.167	0.004
		5th	0.172	0.153	0.168	0.170	0.166	0.007
45	90	1st	0.138	0.111	0.122	0.122	0.123	0.010
		2nd	0.134	0.120	0.110	0.129	0.123	0.009
		3rd	0.129	0.114	0.117	0.125	0.121	0.006
		4th	0.123	0.120	0.118	0.123	0.121	0.002
		5th	0.123	0.122	0.120	0.123	0.122	0.001
90	0	1st	0.125	0.082	0.082	0.116	0.101	0.020
		2nd	0.105	0.098	0.097	0.103	0.101	0.003
		3rd	0.116	0.094	0.092	0.104	0.102	0.010
		4th	0.110	0.092	0.100	0.110	0.103	0.008
		5th	0.105	0.098	0.105	0.103	0.103	0.003
90	45	1st	0.123	0.110	0.110	0.123	0.117	0.007
		2nd	0.129	0.113	0.103	0.123	0.117	0.010
		3rd	0.128	0.091	0.107	0.128	0.114	0.016
		4th	0.128	0.110	0.107	0.110	0.114	0.008
		5th	0.134	0.110	0.110	0.110	0.116	0.010
90	90	1st	0.149	0.108	0.146	0.147	0.138	0.017
		2nd	0.137	0.137	0.137	0.137	0.137	0.000
		3rd	0.147	0.137	0.111	0.143	0.135	0.014
		4th	0.147	0.125	0.132	0.135	0.135	0.008
		5th	0.144	0.132	0.122	0.141	0.135	0.009
135	90	1st	0.149	0.140	0.138	0.142	0.142	0.004
		2nd	0.145	0.139	0.140	0.143	0.142	0.002
		3rd	0.147	0.143	0.142	0.145	0.144	0.002
		4th	0.145	0.138	0.142	0.145	0.143	0.003
		5th	0.145	0.140	0.138	0.143	0.142	0.003

Table B.4 Measurement results of stylus tip wear at four directions on Phu Phan sandstone.

α (degrees)	θ (degrees)	Lines	d (mm)					
			Front	Left	Right	Back	Average	SD
0	-	1st	0.159	0.105	0.156	0.150	0.143	0.022
		2nd	0.156	0.143	0.126	0.152	0.144	0.012
		3rd	0.169	0.110	0.131	0.157	0.142	0.023
		4th	0.150	0.129	0.138	0.150	0.142	0.009
		5th	0.152	0.137	0.128	0.149	0.142	0.010
45	90	1st	0.101	0.101	0.097	0.101	0.100	0.002
		2nd	0.101	0.098	0.097	0.100	0.099	0.002
		3rd	0.101	0.098	0.101	0.101	0.100	0.001
		4th	0.101	0.098	0.097	0.101	0.099	0.002
		5th	0.101	0.101	0.101	0.101	0.101	0.000
90	0	1st	0.085	0.082	0.082	0.082	0.083	0.001
		2nd	0.082	0.082	0.082	0.082	0.082	0.000
		3rd	0.088	0.077	0.076	0.088	0.082	0.006
		4th	0.086	0.077	0.077	0.086	0.082	0.005
		5th	0.086	0.077	0.077	0.077	0.079	0.004
90	45	1st	0.092	0.089	0.089	0.092	0.091	0.002
		2nd	0.096	0.084	0.084	0.096	0.090	0.006
		3rd	0.091	0.091	0.088	0.091	0.090	0.001
		4th	0.094	0.094	0.091	0.091	0.093	0.002
		5th	0.094	0.091	0.080	0.091	0.089	0.005
90	90	1st	0.108	0.105	0.098	0.105	0.104	0.004
		2nd	0.114	0.091	0.108	0.108	0.105	0.009
		3rd	0.107	0.098	0.104	0.107	0.104	0.004
		4th	0.113	0.098	0.095	0.113	0.105	0.008
		5th	0.108	0.103	0.103	0.108	0.106	0.003
135	90	1st	0.111	0.101	0.111	0.111	0.109	0.004
		2nd	0.110	0.106	0.107	0.108	0.108	0.001
		3rd	0.111	0.106	0.111	0.111	0.110	0.002
		4th	0.113	0.100	0.108	0.111	0.108	0.005
		5th	0.110	0.100	0.108	0.108	0.107	0.004

Table B.5 Measurement results of stylus tip wear at four directions on Tak Fa gypsum.

α (degrees)	θ (degrees)	Lines	d (mm)					
			Front	Left	Right	Back	Average	SD
0	-	1st	0.037	0.032	0.034	0.036	0.035	0.002
		2nd	0.040	0.036	0.024	0.038	0.035	0.006
		3rd	0.039	0.030	0.030	0.039	0.035	0.005
		4th	0.040	0.030	0.032	0.036	0.035	0.004
		5th	0.039	0.025	0.035	0.038	0.034	0.006
45	90	1st	0.040	0.040	0.033	0.040	0.038	0.003
		2nd	0.040	0.030	0.040	0.040	0.038	0.004
		3rd	0.039	0.034	0.033	0.036	0.036	0.002
		4th	0.040	0.033	0.036	0.037	0.037	0.003
		5th	0.040	0.039	0.037	0.039	0.039	0.001
90	0	1st	0.030	0.025	0.024	0.025	0.026	0.002
		2nd	0.035	0.025	0.024	0.025	0.027	0.004
		3rd	0.025	0.025	0.021	0.025	0.024	0.002
		4th	0.025	0.022	0.022	0.025	0.024	0.002
		5th	0.025	0.025	0.025	0.025	0.025	0.000
90	45	1st	0.033	0.031	0.031	0.031	0.032	0.001
		2nd	0.037	0.031	0.030	0.036	0.034	0.003
		3rd	0.028	0.028	0.028	0.028	0.028	0.000
		4th	0.033	0.028	0.030	0.033	0.031	0.002
		5th	0.040	0.025	0.028	0.033	0.032	0.006
90	90	1st	0.040	0.040	0.040	0.040	0.040	0.000
		2nd	0.040	0.040	0.040	0.040	0.040	0.000
		3rd	0.040	0.040	0.040	0.040	0.040	0.000
		4th	0.040	0.040	0.040	0.040	0.040	0.000
		5th	0.040	0.037	0.039	0.040	0.039	0.001
135	90	1st	0.051	0.045	0.043	0.046	0.046	0.003
		2nd	0.062	0.037	0.042	0.052	0.048	0.010
		3rd	0.046	0.033	0.042	0.042	0.041	0.005
		4th	0.042	0.040	0.040	0.042	0.041	0.001
		5th	0.042	0.041	0.041	0.042	0.042	0.001

APPENDIX C

SCRATCHING FORCES

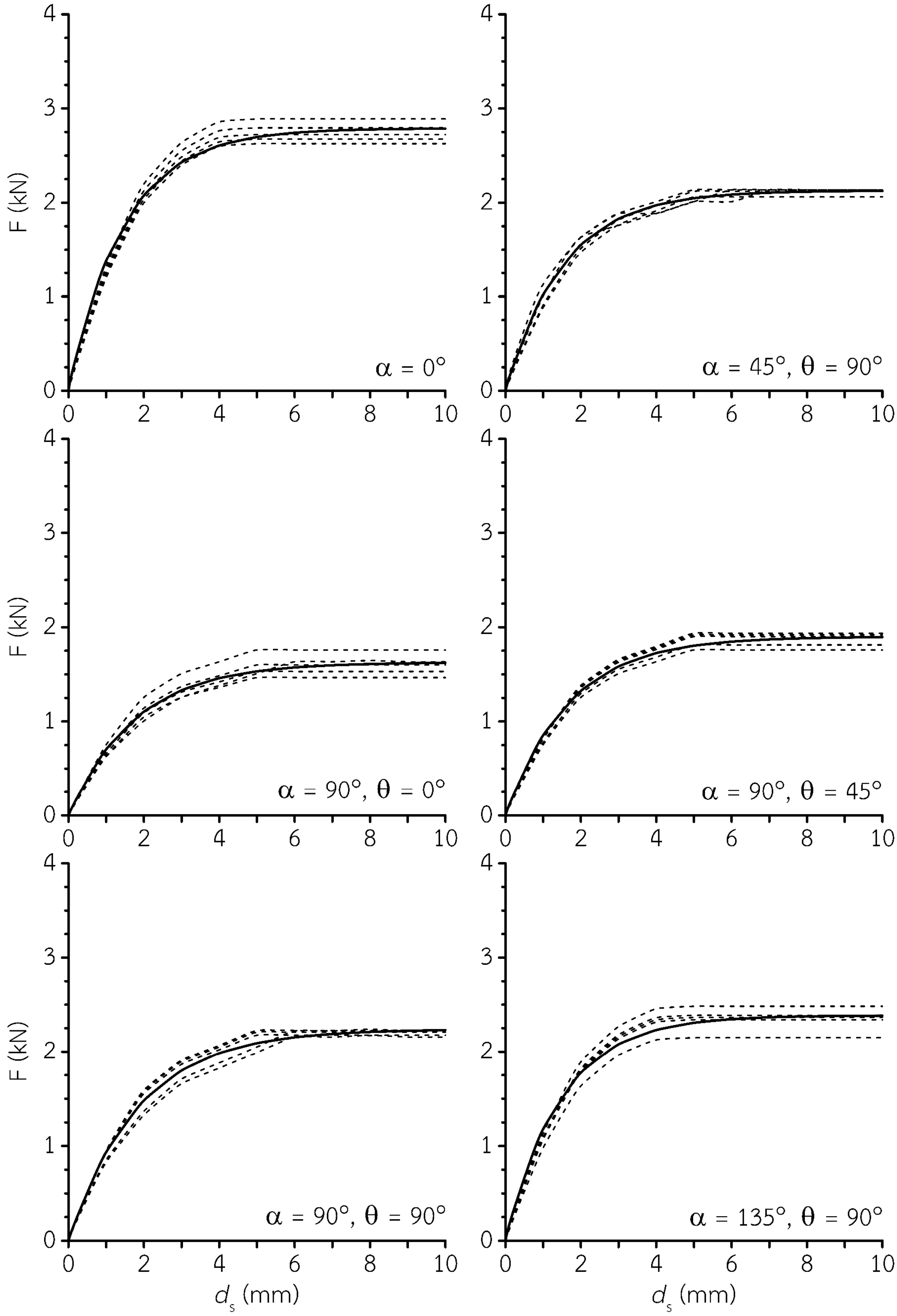

Figure C.1 Scratching forces (F) as a function of scratching displacement (d_s) for Khao Khad argillaceous limestone. Dash line represents each groove. Solid lines are their average.

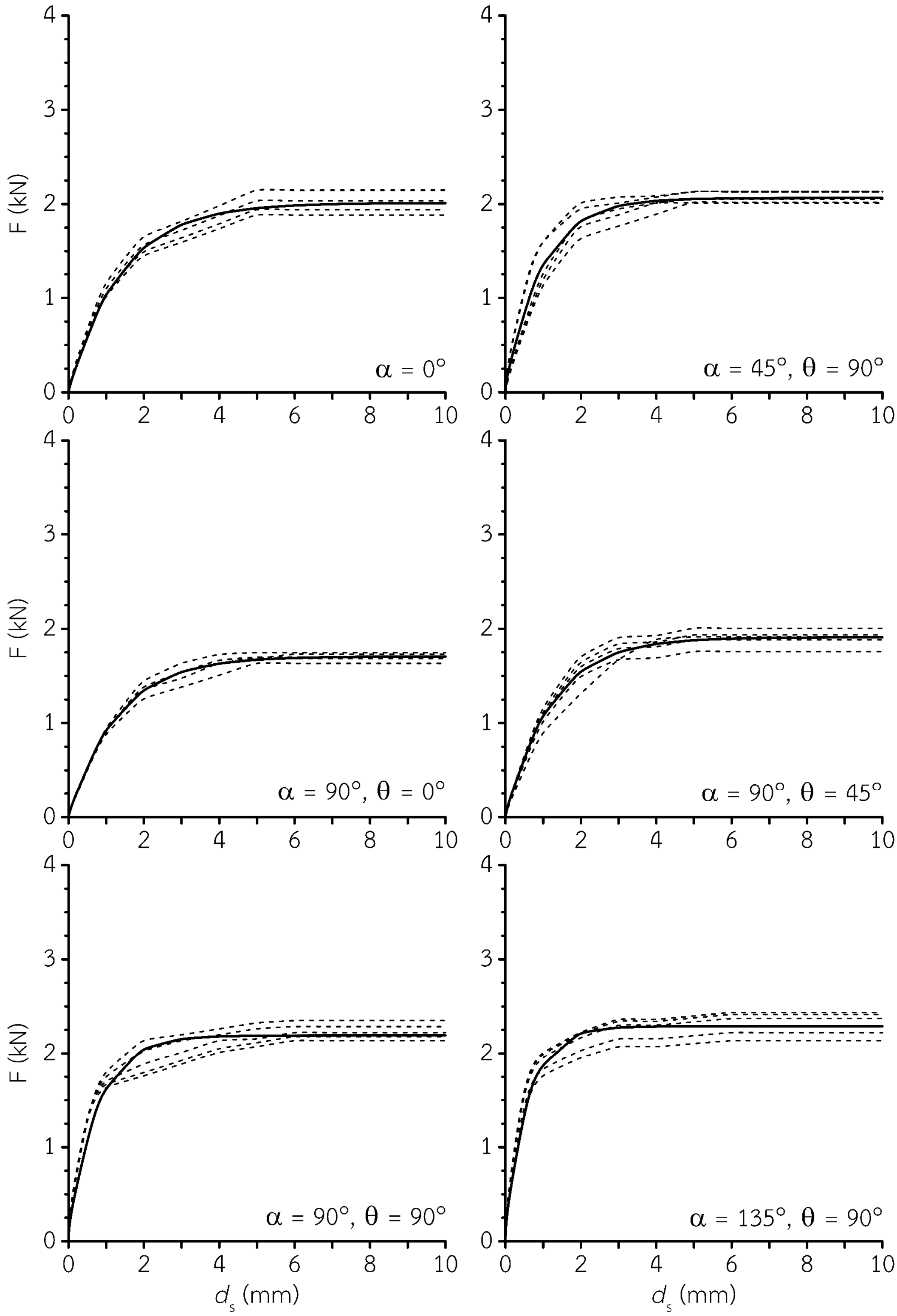

Figure C.2 Scratching forces (F) as a function of scratching displacement (d_s) for Khao Khad bedded limestone. Dash line represents each groove. Solid lines are their average.

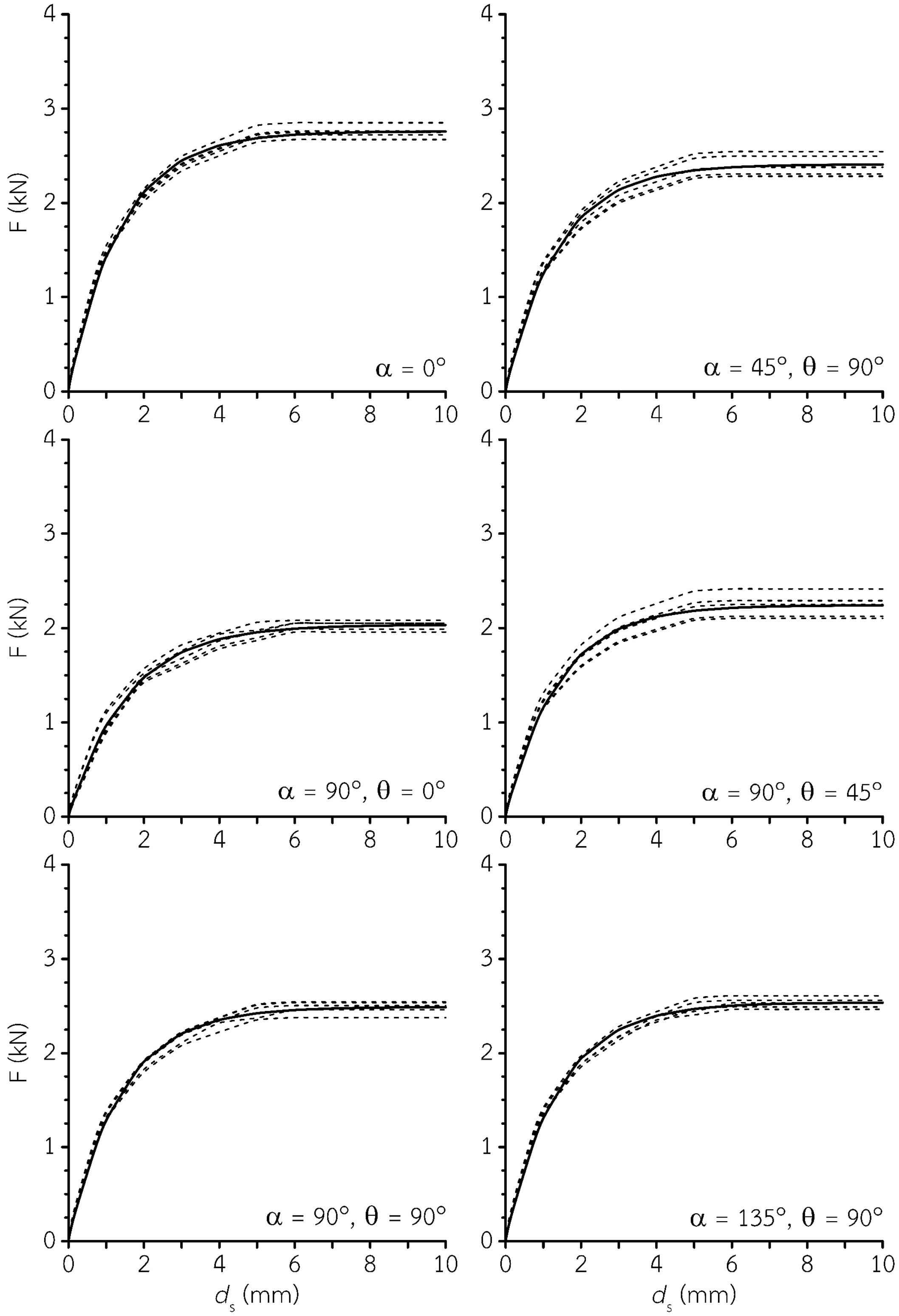

Figure C.3 Scratching forces (F) as a function of scratching displacement (d_s) for Phu Kadueng sandstone. Dash line represents each groove. Solid lines are their average.

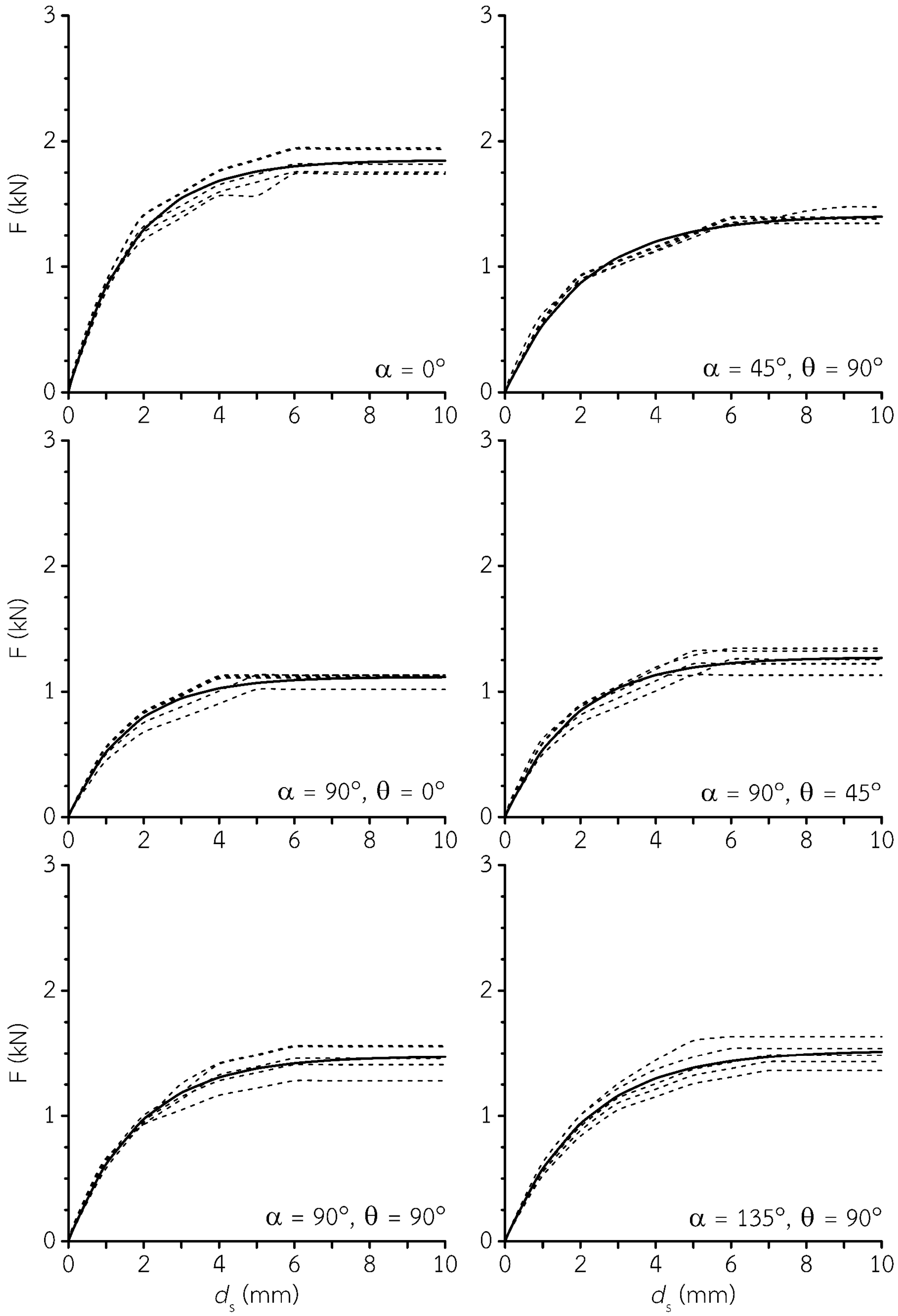

Figure C.4 Scratching forces (F) as a function of scratching displacement (d_s) for Phu Phan sandstone. Dash line represents each groove. Solid lines are their average.

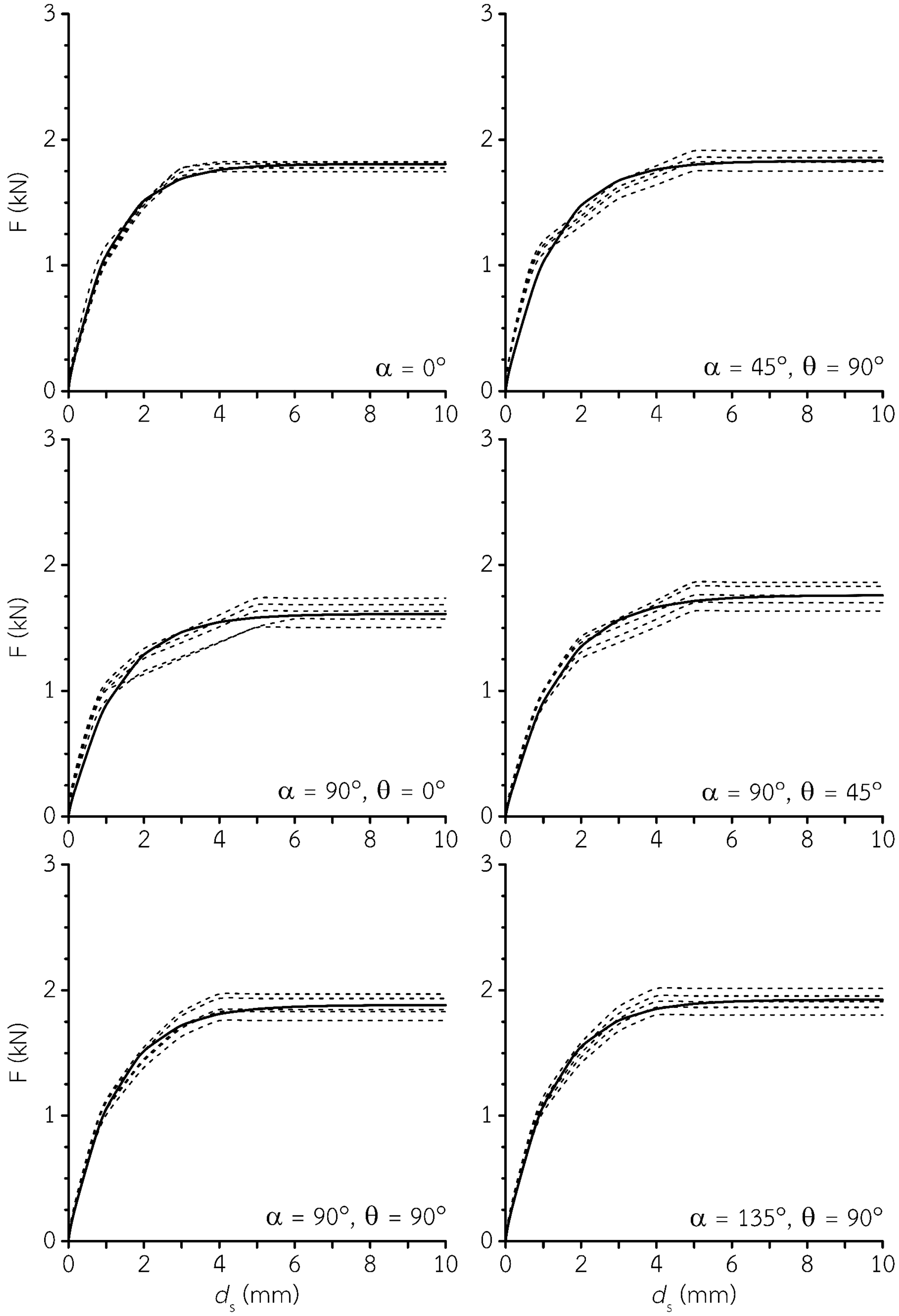

Figure C.5 Scratching forces (F) as a function of scratching displacement (d_s) for Tak Fa gypsum. Dash line represents each groove. Solid lines are their average.

APPENDIX D

LASER - SCANNED IMAGES

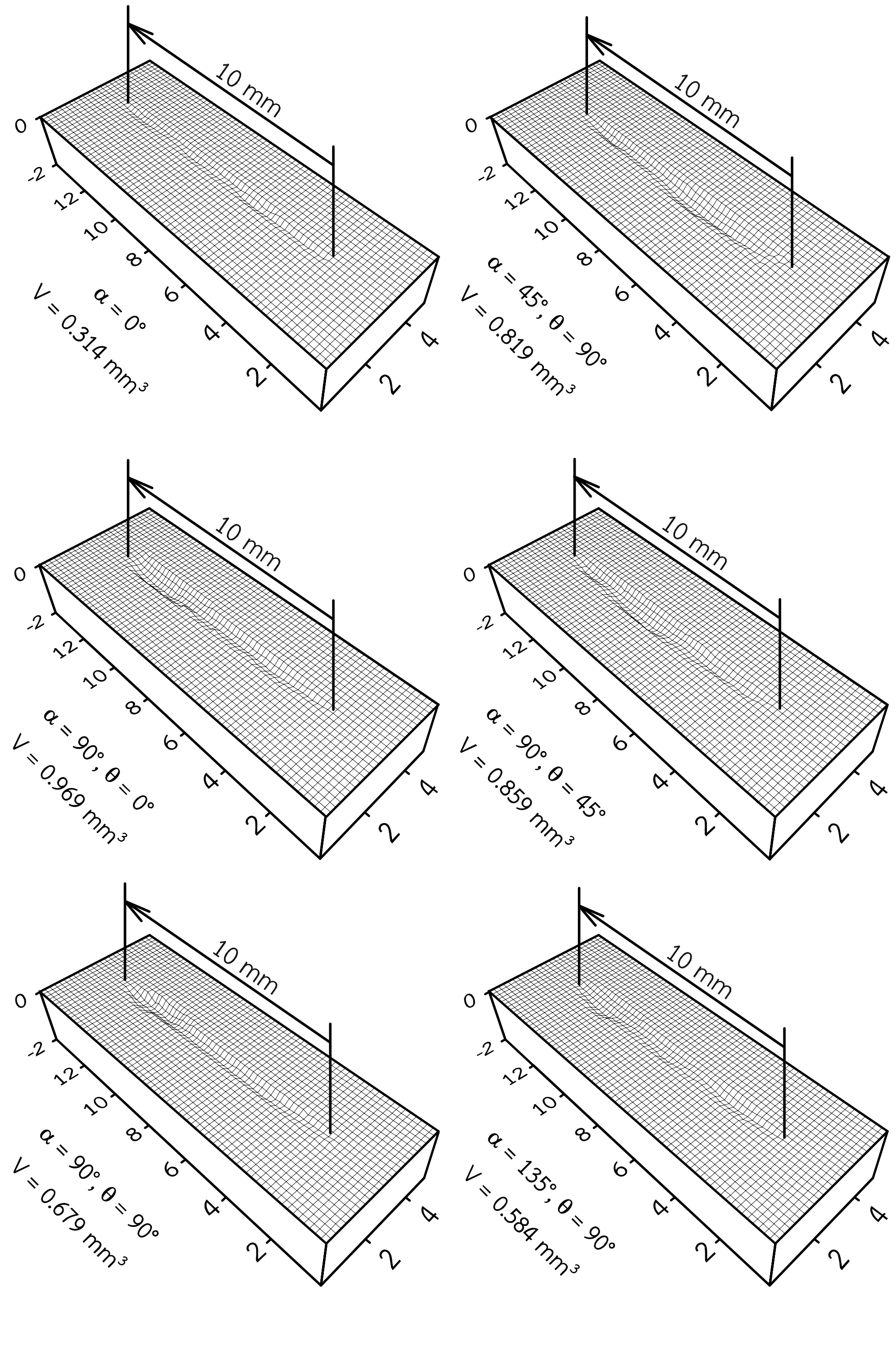

Figure D.1 Groove volume after CERCHAR testing on Khao Khad argillaceous limestone specimens vary bedding plane orientations and scratching directions.

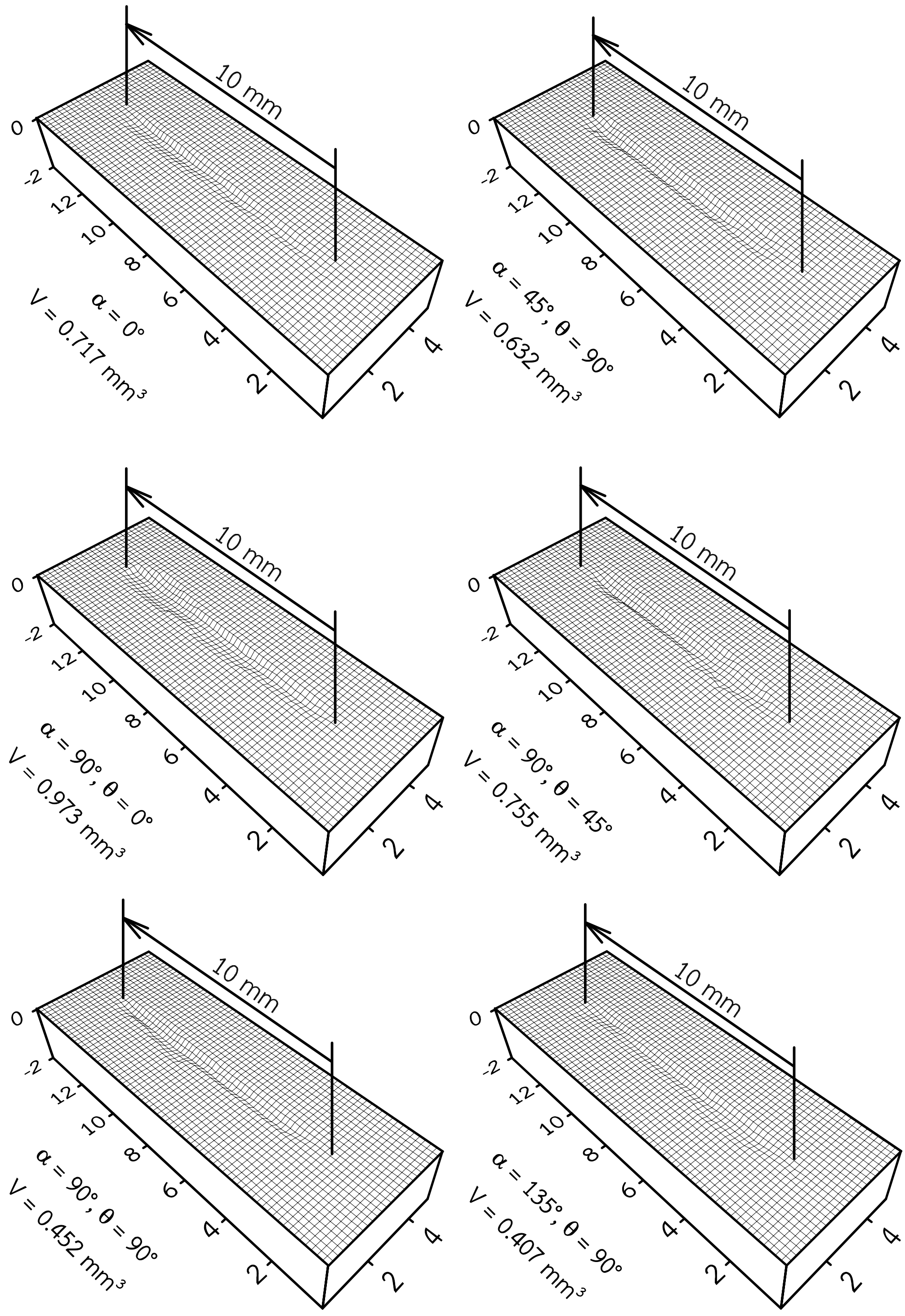

Figure D.2 Groove volume after CERCHAR testing on Khao Khad bedded limestone specimens vary bedding plane orientations and scratching directions.

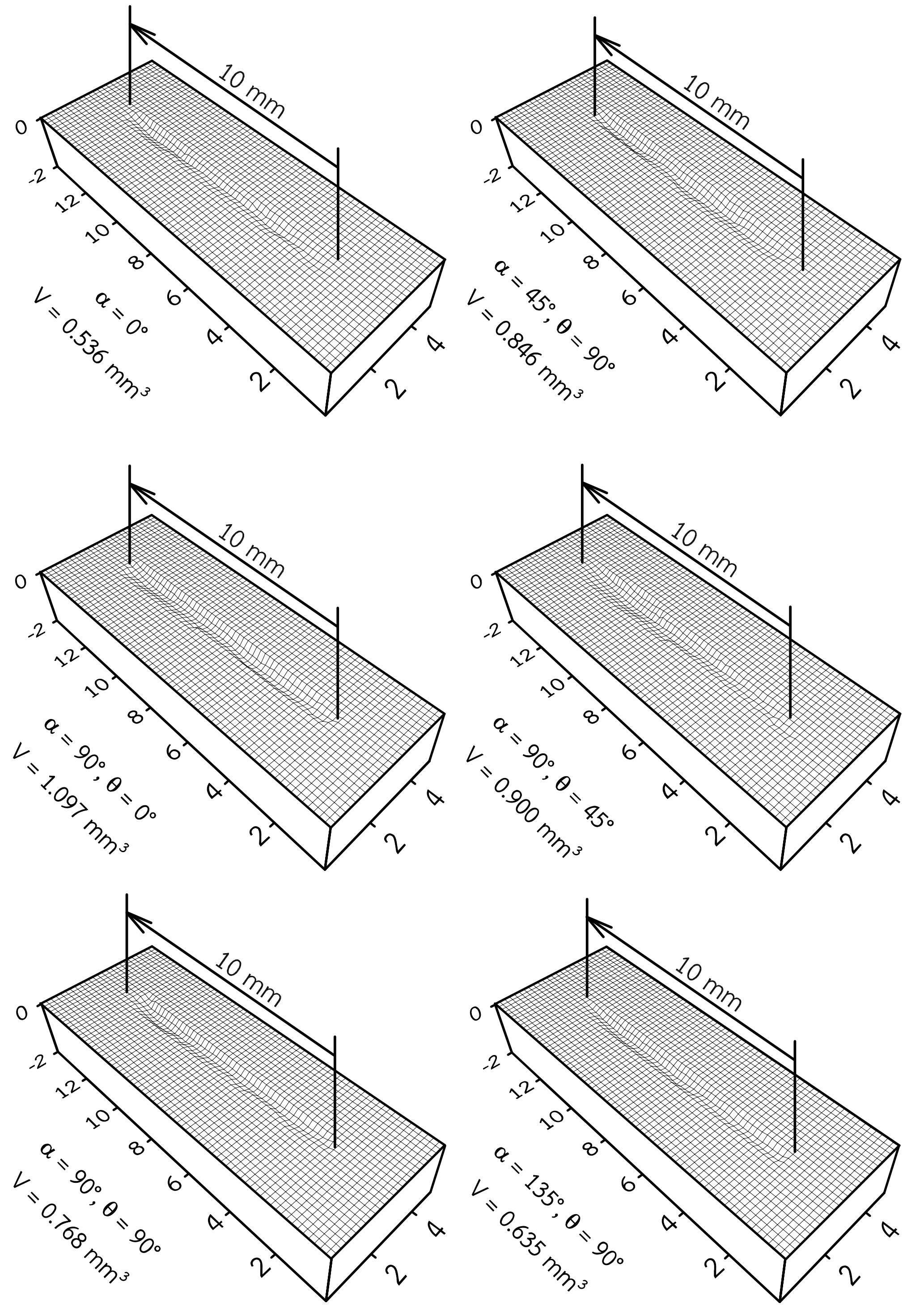

Figure D.3 Groove volume after CERCHAR testing on Phu Kadueng sandstone specimens vary bedding plane orientations and scratching directions.

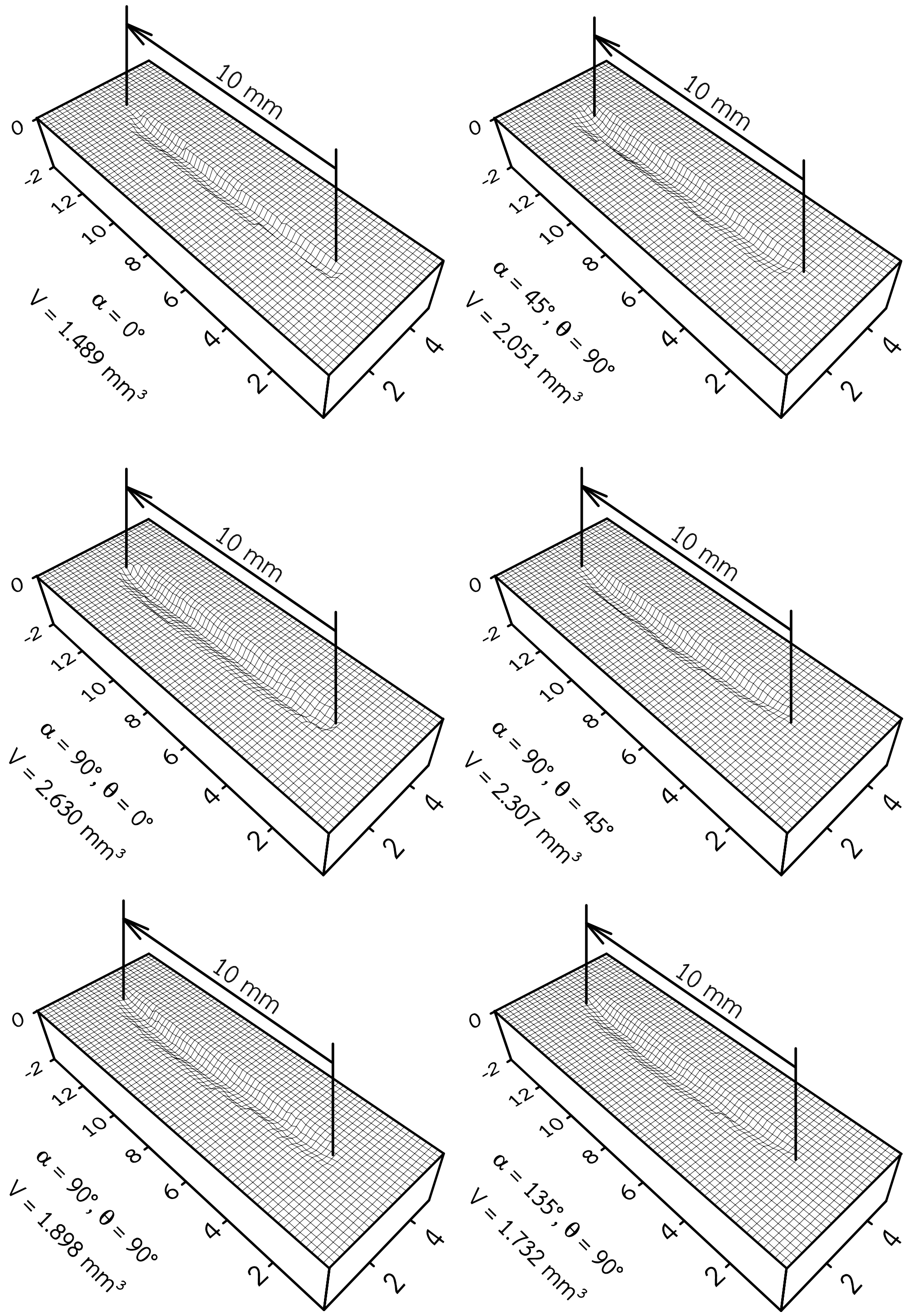

Figure D.4 Groove volume after CERCHAR testing on Phu Phan sandstone specimens vary bedding plane orientations and scratching directions.

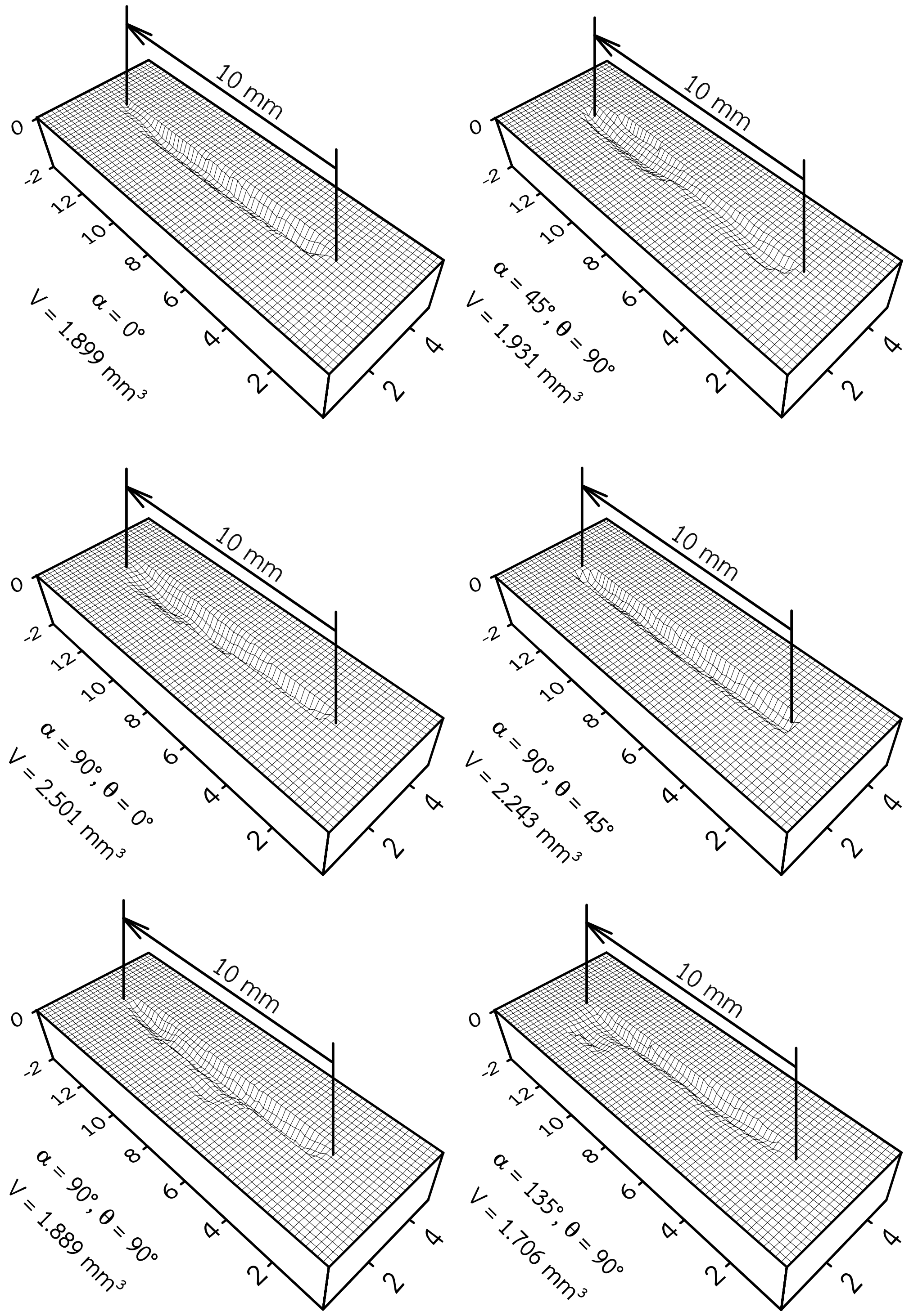

Figure D.5 Groove volume after CERCHAR testing on Tak Fa gypsum specimens vary bedding plane orientations and scratching directions.

APPENDIX E

LIST OF PUBLICATION

Effect of Bedding Plane Orientations and Scratching Directions on CERCHAR Abrasivity Index of Soft to Medium-hard Rocks

Thiti Patcharaarpakul(✉), Laksikar Sitthimongkol, Kittitep Fuenkajorn, and Thanittha Thongprapha

Geomechanics Research Unit, Suranaree University of Technology, Nakhon Ratchasima 30000, Thailand
thiti.b6110819@gmail.com

Abstract. The objective of this study is to determine the effects of bedding plane orientations and scratching directions on the CERCHAR Abrasivity Index (*CAI*) of various rock types, including Khao Khad argillaceous limestone, Khao Khad bedded limestone, Phu Kadueng sandstone, Phu Phan sandstone and Tak Fa gypsum. The ploughing forces and groove volumes are also investigated. The results indicate that higher *CAI* values and ploughing forces are observed in stronger rocks (limestones and sandstones) compared to softer rocks (gypsum). The groove volume increases as the *CAI* value decreases for all tested specimens. Higher *CAI* values are obtained for hard rocks when the scratching direction is opposite to the dip direction of the bedding planes. The highest *CAI* values are observed when the stylus pin moves perpendicular to the bedding trend, rather than along the bedding planes. The effect of bedding plane orientation on *CAI* is more pronounced in strong rocks than in soft ones. These findings will play an important role in maintaining drill bit lifetime, especially within rock types with varying bedding planes.

Keywords: Stylus pin · Abrasiveness · Ploughing force · Groove volume

1 Introduction

Assessing rock properties and steel durability is important for determining the lifespan of cutting tools in construction and excavation industries [1]. Abrasivity testing evaluates tool durability against wear from rock surfaces. CERCHAR abrasivity index (*CAI*) is one of the methods that have been widely used. Several researchers have identified various factors affecting the *CAI*, such as stylus hardness [2, 3], scratching rate [4, 5], scratching distance [6–8], surface condition [6, 9, 10], moisture content [4, 7, 8], temperature [4, 7, 8, 11–13], and rock properties [3, 14, 15]. Bedding planes, which are inherent stratifications within sedimentary rocks, may also considerably affect their abrasivity [16, 17]. Numerous tests on anisotropic rock properties have demonstrated that anisotropic characteristics significantly affecting rock strength results, with maximum rock strengths typically observed at bedding plane orientations of 0° and 90°, and minimum values

T. Kang and Y. Lee (Eds.): ICCEA 2024, LNCE 640, pp. 338–347, 2025.
https://doi.org/10.1007/978-981-96-6115-2_28

between 45° and 60° [17–19]. The effect of bedding planes and their orientations on the abrasiveness of cutting tools has rarely been investigated.

The objective of this study is to determine the effects of bedding plane orientations and scratching directions on the abrasivity of some sedimentary rocks. Crystalline and clastic rocks in Thailand are used as rock samples. The *CAI* test method follows the ASTM D7625-22 standard practice [20].

2 Samples Preparation

Rock samples used in this study are Khao Khad argillaceous limestone, Khao Khad bedded limestone, Phu Kadueng sandstone, Phu Phan sandstone, and Tak Fa gypsum. These rocks are subjected to various excavation tools in mining and construction industry. The test surfaces are cut flat with length-to-diameter (*L*/*D*) ratio of 1. The nominal angles (α) between the test surface and bedding plane vary from 0°, 45°, 90° to 135°. The scratching directions of the stylus pin with respect to the bedding trends vary from 0° to 90°. The specimens are oven-dried before testing. Table 1 shows bedding plane characteristics of the test samples.

Table 1. Bedding plane characteristics.

Rock type	Bedding plane characteristics
Khao Khad argillaceous limestone	Bedding planes can be observed by the alternation of gray limestone and pale brown clay bands, with average thickness of 1 mm.
Khao Khad bedded limestone	Bedding planes can be observed by the alternation of gray limestone and white calcite bands, with average thickness of 0.5 mm.
Phu Kadueng sandstone	Bedding planes can be observed by the alternation of pale green quartz and black biotite bands, with average thickness of 1.5 mm.
Phu Phan sandstone	Bedding planes can be observed by the alternation of pale red quartz and red microcline bands, with average thickness of 1 mm.
Tak Fa gypsum	Bedding planes can be observed by the alternation of white gypsum and gray anhydrite bands, with average thickness of 2 mm.

3 Test Method

The test method and calculation follow ASTM D7625-22 standard practice [20]. Two test series are performed to determine the effects of bedding plane orientation (α) and scratching direction (θ), as shown in Fig. 1. CERCHAR testing is conducted on saw-cut surfaces with varying bedding plane angles using a device based on the West apparatus, as shown in Fig. 2. The wear on the stylus tip is measured under a microscope with 50 times magnification. Five pins are used per bedding plane angle. Ploughing force on the stylus is calculated from the torque applied to the hand crank as follows (Eq. 1):

$$F = 2\pi T/P \tag{1}$$

where F represents ploughing force (N), T denotes torque (N·m) applied on the crank, and P is screw pitch (0.001 mm). Groove volume produced by scratching on specimen surface are measured by laser-scanning with a 0.1 mm line scan interval and vertical precision of $\pm$ 1 micron. The results are used to calculate the groove volume by using SURFER software.

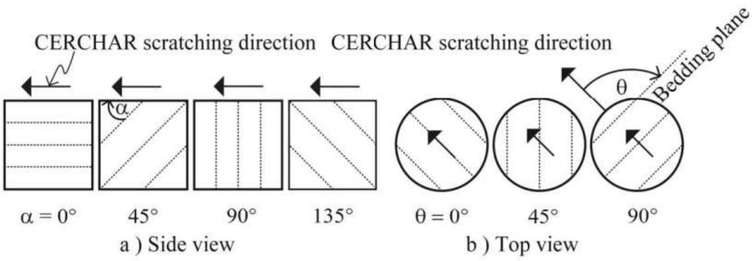

Fig. 1. Scratching direction as compound to bedding plane angles (a), and as compared to trends of bedding planes (b).

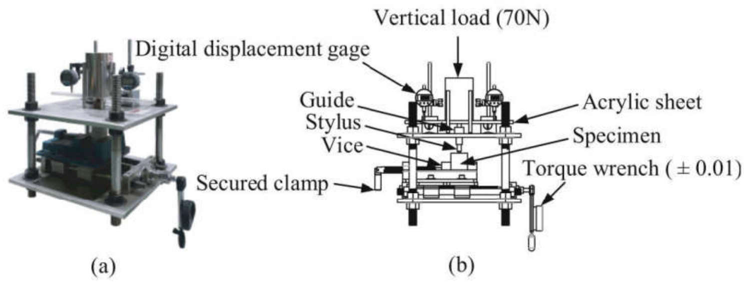

Fig. 2. Device based on West CERCHAR apparatus with additional torque measurements (a) schematic drawing of CERCHAR device (b) [15].

4 Results

4.1 CERCHAR Abrasivity Index

Bedding plane angle (α) and scratching direction (θ) do affect the wear of stylus pins. Table 2 presents *CAI* results for all boundary conditions. Based on ASTM D7625-22 [20] these rocks are classified as medium to high abrasiveness, except for Tak Fa gypsum where it is classified as very low abrasiveness regarding of scratching direction and bedding plane angle. For all bedding plane orientations, Khao Khad argillaceous limestone has the highest *CAI*, while Tak Fa gypsum has the lowest *CAI* values.

The *CAI* varies with α angle, as shown in Fig. 3a. For the argillaceous limestone, the *CAI* is highest at $\alpha = 0°$ and lowest at $\alpha = 45°$. Similar trends are observed for Phu Kadueng and Phu Phan sandstones. The bedded limestone and Tak Fa gypsum show the highest *CAI* at $\alpha = 135°$ and the lowest at $\alpha = 0°$. The *CAI* increases slightly with θ angle, peaking at $\theta = 90°$ and reaching its lowest value at $\theta = 0°$ for all tested rocks (Fig. 3b).

4.2 Groove Volume

The groove volume obtained from laser 2-D scanner is consistent with the *CAI* values. It increases as the *CAI* value decreases. Table 2 gives groove volumes for all boundary conditions. Largest volumes are obtained for $\alpha = 45°$. This is true for all tested specimens. For $\alpha = 90°$, largest groove volume can be observed when the pin direction is parallel to the bedding trends ($\theta = 0°$). Soft rocks (e.g. gypsum) show largest groove volume, as

Table 2. CERCHAR abrasivity index and groove volume with different bedding plane orientations.

Rock type	α (degrees)	θ (degrees)	*CAI*	Abrasiveness index	Volume (mm^3)
Khao Khad argillaceous limestone	0	–	2.54 ± 0.11	High	0.314 ± 0.03
	45	90	1.86 ± 0.02	Medium	0.819 ± 0.06
	90	0	1.61 ± 0.01	Medium	0.969 ± 0.04
	90	45	1.76 ± 0.01	Medium	0.859 ± 0.05
	90	90	1.99 ± 0.04	Medium	0.679 ± 0.05
	135	90	2.20 ± 0.00	High	0.584 ± 0.04
Khao Khad bedded limestone	0	–	1.17 ± 0.00	Medium	0.717 ± 0.02
	45	90	1.20 ± 0.01	Medium	0.632 ± 0.04
	90	0	1.07 ± 0.01	Medium	0.973 ± 0.06
	90	45	1.10 ± 0.00	Medium	0.755 ± 0.03
	90	90	1.26 ± 0.00	Medium	0.452 ± 0.02
	135	90	1.28 ± 0.01	Medium	0.407 ± 0.07
Phu Kadueng sandstone	0	–	1.90 ± 0.01	Medium	0.536 ± 0.03
	45	90	1.39 ± 0.01	Medium	0.846 ± 0.10
	90	0	1.16 ± 0.01	Medium	1.097 ± 0.05
	90	45	1.32 ± 0.01	Medium	0.900 ± 0.05

(*continued*)

Table 2. (*continued*)

Rock type	α (degrees)	θ (degrees)	*CAI*	Abrasiveness index	Volume (mm^3)
	90	90	1.55 ± 0.01	Medium	0.768 ± 0.08
	135	90	1.63 ± 0.01	Medium	0.635 ± 0.04
Phu Phan sandstone	0	–	1.63 ± 0.01	Medium	1.489 ± 0.10
	45	90	1.13 ± 0.00	Medium	2.051 ± 0.04
	90	0	0.93 ± 0.00	Low	2.630 ± 0.12
	90	45	1.03 ± 0.01	Medium	2.307 ± 0.05
	90	90	1.19 ± 0.00	Medium	1.898 ± 0.03
	135	90	1.24 ± 0.01	Medium	1.732 ± 0.08
Tak Fa gypsum	0	–	0.40 ± 0.00	Very low	1.899 ± 0.06
	45	90	0.43 ± 0.01	Very low	1.931 ± 0.05
	90	0	0.29 ± 0.01	Very low	2.501 ± 0.04
	90	45	0.36 ± 0.02	Very low	2.243 ± 0.03
	90	90	0.45 ± 0.00	Very low	1.889 ± 0.07
	135	90	0.50 ± 0.03	Very low	1.706 ± 0.06

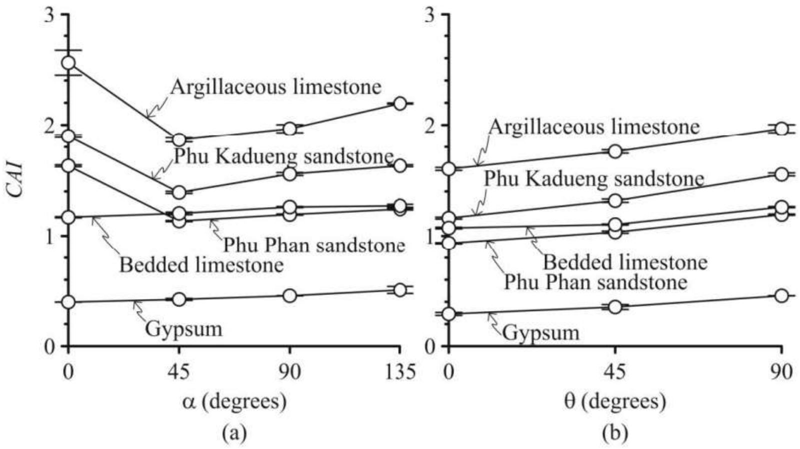

Fig. 3. *CAI* as a function of bedding plane angle (a), and scratching direction (b).

compared to the stronger ones (e.g. limestones), as shown in Fig. 4. Similar trends are observed for Phu Kadueng and Phu Phan sandstone. Gypsum and bedded limestone have the highest groove volume at α = 0° and the lowest at α = 135°. As shown in Fig. 4b, groove volume increases with the θ angle, peaking at $\theta = 90°$ and reaching its lowest at $\theta = 0°$ for all tested rocks. Phu Phan sandstone and Tak Fa gypsum show similar groove volume despite their different levels of abrasiveness.

4.3 Ploughing Force

An empirical equation is proposed to represent F as a function of d_s:

$$F = a \cdot (1 - exp \cdot (-b \cdot d_s)) \qquad (2)$$

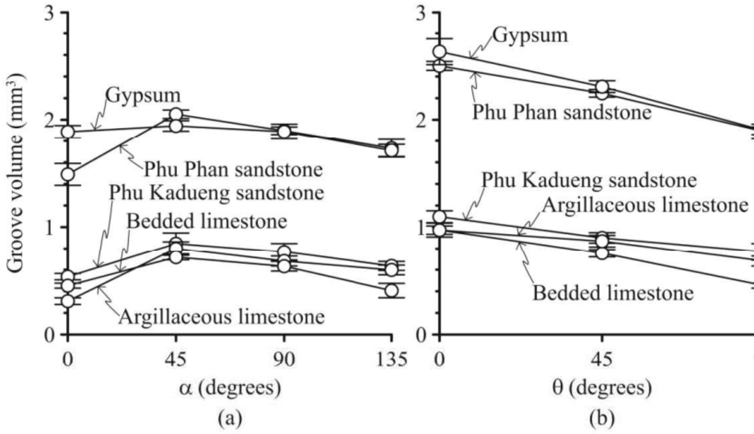

Fig. 4. Groove volume as a function of bedding plane angle (a), and scratching direction (b).

where a and b are empirical constants depending on rock types, as shown in Table 3. Good correlations are obtained for all boundary conditions ($R^2 > 0.9$). Figs. 5 and 6 shows examples of ploughing force as a function of scratching distance for different α and θ angles, respectively. They increase rapidly within the first 2-4 mm and then trend to approach constant magnitudes. Stronger rocks (limestones) show higher ploughing forces than the soft ones (gypsum), regarding of α and θ angles. Highest force is observed from $\alpha = 0°$ with the lowest at 45° and 90°. The differences vary from 5% (soft rocks) to 15% (strong rocks). For scratching direction with $\theta = 0°$, larger difference is observed from strong rocks, as compared to those of soft rocks. This implies that the effects of bedding plane orientations and scratching directions are pronounced more in strong rocks than in soft rocks.

5 Discussions

The agreements between CAI, F and V for all rocks and boundary conditions confirm that the results of testing are correct. The higher CAI and F with lower groove volume are observed for strong rocks as compared to soft rocks.

Higher *CAI* values are obtained for both crystalline and clastic rocks when the scratching direction is opposite to the dip direction (α) of bedding plane. Under this condition, the alternation of soft and hard layers show the largest effect on the stylus wear. On the contrary, if the scratching direction is the same with bedding plane dip angle, the wear of stylus pins (*CAI*) becomes lower. This also results in a lower *CAI* and ploughing force, F, with higher scratching volume. This also agrees with the results obtained from the effects of scratching direction that largest *CAI*, *F* and *V* values are observed when the stylus pin moves perpendicular to the bedding trend (θ = 90°).

Table 3. Empirical constants *a* and *b* for F-d_s relation and R^2.

Rock type	α (degrees)	θ (degrees)	$F = a \cdot (1 - exp \cdot (- b \cdot d_s))$		R^2
			a (N)	b (m^{-1})	
Khao Khad argillaceous limestone	0	–	2.789	0.682	0.986
	45	90	2.128	0.654	0.993
	90	0	1.627	0.568	0.950
	90	45	1.899	0.598	0.987
	90	90	2.240	0.541	0.989
	135	90	2.386	0.682	0.977
Khao Khad bedded limestone	0	–	2.012	0.719	0.979
	45	90	2.064	1.062	0.977
	90	0	1.707	0.777	0.990
	90	45	1.909	0.827	0.977
	90	90	2.192	1.339	0.970
	135	90	2.289	1.694	0.970
Phu Kadueng sandstone	0	–	2.759	0.728	0.995
	45	90	2.409	0.728	0.982
	90	0	2.036	0.646	0.989
	90	45	2.242	0.728	0.976
	90	90	2.491	0.724	0.993
	135	90	2.538	0.723	0.995
Phu Phan sandstone	0	–	1.850	0.603	0.978
	45	90	1.411	0.477	0.989
	90	0	1.118	0.626	0.974
	90	45	1.274	0.549	0.967
	90	90	1.478	0.538	0.963
	135	90	1.525	0.477	0.964

(*continued*)

Table 3. (*continued*)

Rock type	α (degrees)	θ (degrees)	$F = a \cdot (1 - exp \cdot (-b \cdot d_s))$		R^2
			a (N)	*b* (m^{-1})	
Tak Fa gypsum	0	–	1.807	0.912	0.995
	45	90	1.832	0.820	0.982
	90	0	1.611	0.802	0.960
	90	45	1.759	0.730	0.967
	90	90	1.883	0.819	0.983
	135	90	1.925	0.819	0.985

For clastic rocks, the results also imply that scratching across bedding planes through layers with different grain sizes would cause more wear to the stylus pin (higher *CAI*), as compared to that along bedding plans through the same layers of the similar grain size.

For crystalline rocks, the variation of *CAI* would depend on the hardness of the crystallization layers (in this case, calcite). If the hardness of different crystallized layers is the same, the effect of bedding plane would be minimal.

The bedding plane thickness of all rocks tested here is similar (0.5-2 mm). The ef-fect of bedding plane thickness cannot be assessed.

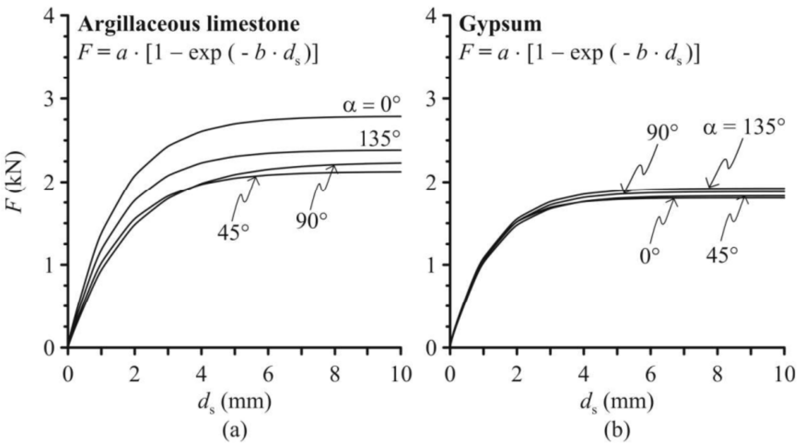

Fig. 5. Scratching force as a function of direction under different bedding plane angles for Khao Khad argillaceous limestone (a), and Tak fa gypsum (b).

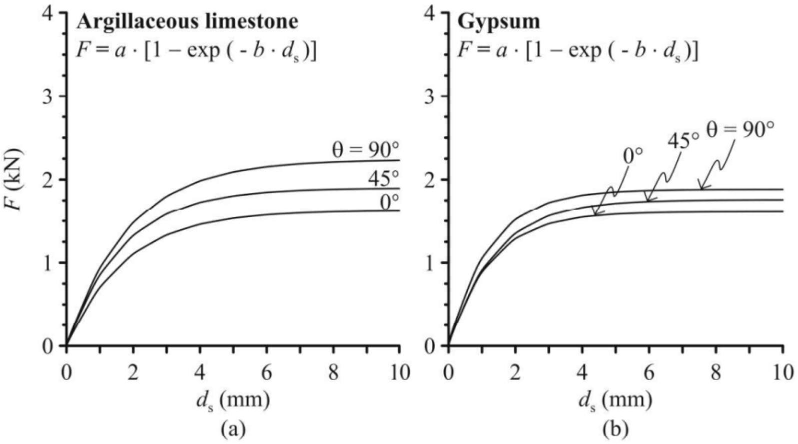

Fig. 6. Scratching force as a function of direction under different scratching directions for Khao Khad argillaceous limestone (a), and Tak fa gypsum (b).

6 Concussion

Results from this study can be concluded, as follows:

- The scratching directions (θ) affect *CAI* and force that does bedding plane orientations (α).
- Bedding plane orientations affect *CAI* of strong rocks more than soft rocks.
- Scratching of stylus pin across bedding planes show larger *CAI* than along bedding planes.

References

1. Rajati, M.H., Rostami, J., Memarian, H., Hamzaban, M.T.: A study on predicting the wear of TBM disc cutters using Cerchar testing. Tunn. Undergr. Space Technol. **140**, 105290 (2023)
2. Yaralı, O., Duru, H.: Investigation into effect of scratch length and surface condition on Cerchar abrasivity index. Tunn. Undergr. Space Technol. **60**, 111–120 (2016)
3. Teymen, A.: The usability of Cerchar abrasivity index for the estimation of mechanical rock properties. Int. J. Rock Mech. Min. Sci. **128**, 104258 (2020)
4. Aydın, H.: Investigating the effects of various testing parameters on Cerchar abrasivity index and its repeatability. Wear **418–419**, 61–74 (2019)
5. Hamzaban, M.T., Karami, B., Rostami, J.: Effect of pin speed on Cerchar abrasion test results. J. Test. Eval. **47**(1), 121–139 (2019)
6. Al Ameen, S.I., Waller, M.D.: The influence of rock strength and abrasive mineral content on the Cerchar Abrasive Index. Eng. Geol. **36**(3), 293–301 (1994)
7. Plinninger, R., Käsling, H., Thuro, K., Spaun, G.: Testing conditions and geomechanical properties influencing the CERCHAR abrasiveness index (CAI) value. Int. J. Rock Mech. Min. Sci. **40**(2), 259–263 (2003)

8. Zhang, G., Konietzky, H., Song, Z., Huang, S.: Study of some testing condition-based factors affecting the Cerchar abrasivity index (CAI). Arab. J. Geosci. **13**(23), 1254 (2020)
9. Aydın, H., Yaralı, O., Duru, H.: The effects of specimen surface conditions and type of test apparatus on Cerchar Abrasivity index. Karaelmas Fen ve Mühendislik Dergisi **6**(2), 293–298 (2016)
10. Hamzaban, M.T., Rostami, J., Dahl, F., Macias, F.J., Jakobsen, P.D.: Wear of cutting tools in hard rock excavation process: a critical review of rock abrasiveness testing methods. Rock Mech. Rock Eng. **56**, 1843–1882 (2022)
11. Rossi, E., Saar, M.O., Rudolf von Rohr, P.: The influence of thermal treatment on rock–bit interaction: a study of a combined thermo–mechanical drilling (CTMD) concept. Geothermal Energy **8**(1), 16 (2020)
12. Ji, Y., Wang, L., Zheng, Y., Wu, W.: Temperature-dependent abrasivity of Bukit Timah granite and implications for drill bit wear in thermo-mechanical drilling. Acta Geotech. **16**(3), 885–893 (2021)
13. Wang, L., Guo, K., Wu, W.: Abrasivity measurement of brittle rock after thermal treatment. Measurement **212**, 112710 (2023)
14. Alber, M.: Stress dependency of the Cerchar abrasivity index (CAI) and its effects on wear of selected rock cutting tools. Tunn. Undergr. Space Technol. **23**(4), 351–359 (2008)
15. Kathancharoen, N., Fuenkajorn, K.: Effects of mechanical and mineralogical properties on CERCHAR abrasivity index and specific energy of some Thai rocks. Eng. Appl. Sci. Res. **50**(5), 478–489 (2023)
16. Ramamurthy, T.: Strength and Modulus Responses of Anisotropic Rocks. Pergamon, Oxford (1993)
17. Gholami, R., Rasouli, V.: Mechanical and elastic properties of transversely isotropic slate. Rock Mech. Rock Eng. **47**, 1763–1773 (2014)
18. Al-Harthi, A.A.: Effect of planar structures on the anisotropy of Ranyah sandstone, Saudi Arabia. Eng. Geol. **50**(1), 49–57 (1998)
19. Sukjaroen, N., Thongprapha, T., Liabkrathok, P., Fuenkajorn, K.: Effects of loading rate on transverse isotropic responses of bedded gypsum. Arab. J. Geosci.Geosci. **14**(22), 2442 (2021)
20. ASTM D7625-22.: Standard Test Method for Laboratory Determination of Abrasiveness of Rock Using the CERCHAR Abrasiveness Index Method. West Conshohocken, PA (2022)